RZ 3016 (# 93062) 04/20/98
Physical Sciences & Chemistry 42 pages

Research Report

Fullerenes and Silicon Clusters: Structures, Electronic Properties, and Dynamics

Wanda Andreoni

IBM Research Division
Zurich Research Laboratory
8803 Rüschlikon
Switzerland

IBM Research Division
Almaden · Austin · Beijing · Haifa · T.J. Watson · Tokyo · Zurich

Fullerenes and Silicon Clusters: Structures, Electronic Properties, and Dynamics

Wanda Andreoni

IBM Research Division, Zurich Research Laboratory, 8803 Rüschlikon, Switzerland

Abstract

In these lectures I wish to give a brief and critical overview of the state-of-the-art calculations of the structural, electronic, and dynamical properties of fullerenes and clusters, with emphasis on fullerene derivatives and silicon clusters. The accent will be on the comparison of different methods and especially on the comparison of theory and experiment.

Regarding fullerenes: I enclose two recent reviews, one that will appear in *Annual Review of Physical Chemistry* and one on metallofullerenes currently in press for *Appl. Phys. A*, written in collaboration with Alessandro Curioni.

Regarding silicon clusters: my lectures will be based on published literature (see especially U. Röthlisberger, W. Andreoni, and M. Parrinello, *Phys. Rev. Lett.* **72**, 665–668, 1994) as well as on recent results obtained for their electronic properties. During the past ten years, small silicon clusters have been used as test cases for a number of computational approaches, especially aimed to determine their “equilibrium” structures. In spite of this, the diversity of the proposals that are still accepted and “put forward” for these geometries is striking. Unfortunately there are no experiments that can directly probe the structure of a cluster in beam. I shall, however, present a critical overview of the results of the calculations and of the experimental data available so far on “free” silicon clusters. The discussion of size effects on the electronic properties will be extended to novel silicon-cluster-based materials and also to porous silicon.

FROM: *Annual Review of Physical Chemistry* (1998) in press

COMPUTATIONAL APPROACH TO THE PHYSICAL CHEMISTRY OF FULLERENES AND THEIR DERIVATIVES

Wanda Andreoni

IBM Research Division, Zurich Research Laboratory, CH–8803 Rüschlikon, Switzerland

Abstract: A critical review is presented of results obtained with different computational methods (mainly *ab-initio*) on C_{60}, C_{70}, and specific fullerene derivatives, also in comparison with experimental data. From the discussion of diverse systems, the (often underestimated) complexity of their physical and chemical behavior emerges, and hence the importance of an accurate description and the need for a careful inspection of the experimental data, with which comparison is often intrinsically difficult. The ambition of this review is to help establish a basis not only for a non-superficial reading of the existing literature, but also for a constructive approach with computations to the challenge posed by recent promising applications of fullerenes in nanotechnology, optoelectronics, and biology.

INTRODUCTION

An overview of theoretical approaches to the physical chemistry of fullerenes [1] would certainly occupy an entire book. The purpose of the present survey is more limited: It contains the results of theoretical approaches, mainly "*ab-initio*", to some relevant but specific aspects, and focuses on a critical comparison of theory with experiment and of different computational methods. Regarding the technical aspects of the methods used in the literature, the reader will be referred to appropriate articles. Many aspects of the physics and chemistry of fullerenes are understood by now but many others still constitute an open question. In a number of cases, we seem to have contrasting but still co-existing views. To what extent are results biased by the method used or by the limited investigation made so far? There is a widespread tendency to claim agreement with experiment and also to state a general consistency between different methods. To what extent are we justified in this optimistic but superficial attitude? I hope that appropriate answers and/or suggestions emerge naturally from the sections that follow.

Much has been written about the structure, bonding, optical properties, and dynamics of bare fullerenes, especially about C_{60}. Less is currently available on derivatives obtained by doping and additions. Yet, they are the main focus of fullerene chemistry, and constitute a topic where theory and experiment can indeed complement each other. Thanks to the recent progress in computations, the road for a combined approach to the design of novel, fullerene-based materials is in principle open. However, in order to be able to choose the "right way to go" and to eventually trust the predictive power of calculations, we need a thoughtful reconsideration of the computational work of the past ten years. It is my wish to provide some guide to a nonsuperficial reading of the fullerene literature [2], and stimulus for progress in this research.

C_{60} AND C_{70} MOLECULES

In the past decade, theoretical and computational approaches with diverse degrees of sophistication [3] have been applied to the study of C_{60} and to the calculation of its fundamental properties. A number of methods have also been applied to higher fullerenes, although to a lesser extent, owing to both the lower symmetry of the structure and to the comparative lack of stimulating experiments. This section compares some results on C_{60} and C_{70} obtained with widely used *ab-initio* methods. Only partial reference is given to semi-empirical approaches to their fundamental properties. Although useful in all cases in which *ab-initio* methods become too costly, the lack of accuracy makes their validity as an aid to rational material design highly questionable.

However, the underlying idea of such an exercise is not to either praise or blame one method with respect to the other. My intention is only to clarify which features a specific calculation can or fails to capture, and especially to what extent theory can be compared with experiment.

In C_{60} (Fig. 1(a)), there are two types of bonds: those at the fusion of two hexagonal rings and those at the fusion of one pentagonal and one hexagonal ring. The former is denoted as "double", the latter as "single" bond. The calculated bond orders are in the range of 1.1 to 1.4 [4]. In C_{70} (Fig. 1(b)) the situation is more complex: The inclusion of five additional hexagonal rings lowers the symmetry and splits the bonds into eight inequivalent ones, with bond orders approximately in the same range as those in C_{60}.

Because of the complexity of the systems, most *ab-initio* calculations in the literature use small basis sets for the electronic wavefunctions. To provide a meaningful comparison, only those results are reported for each method that were obtained with the so far best basis set [5, 6]. Tables 1 to 4 quote structural characteristics, first-ionization potentials (IP), electron affinities (EA), and vibrational frequencies. The IPs and EAs values listed are correctly calculated as differences of total energies (ΔSCF) of neutral and charged states.

The results obtained by the Hartree–Fock (HF) method [7] are especially instructive, because its failure or success is a direct measure of the importance of correlation effects (see Table 1). In C_{60} (Table 1), it is apparent that neglecting correlation enhances bond alternation when compared to experimental values [8]. This is a typical result of the HF method, and can be associated with its overestimate of the gap between the highest occupied (HOMO) and the lowest unoccupied molecular orbital (LUMO). It manifests itself in the narrowing of the "double" bonds and in a "broadened" vibrational spectrum caused by a hardening of the high-frequency modes, two features that are related. In fact, while the low-frequency part of the spectrum corresponds to radial modes, the high-frequency part corresponds to tangential vibrations [9], which are more sensitive to the HF shrinking of the "double" bonds. At the MP2 level of theory [10], this shortcoming of the HF method has been partially corrected. Unfortunately, no post-HF calculations of a higher level are available.

In the HF method, the difference between the Koopmans's estimate and the ΔSCF calculation for the vertical IP measures the effect of wavefunction relaxation at fixed structure. The latter is reported to be 0.2–0.3 eV [11]. The vertical IP is thus overestimated by less than 0.5 eV, whereas the EA is dramatically underestimated (see Table 1). The latter result is only in part due to the computational scheme, i.e. the limitation of the wavefunction basis set and the limited accounting for the breaking of symmetry due to the addition of either an electron or a hole. Binding of the extra electron depends critically on the effects of electron correlation. One can expect, therefore, that this affects the validity of HF calculations in describing the reduction properties of C_{60}, which are fundamental to its chemistry.

Density-functional-theory (DFT) [12] has widely been applied to C_{60}, within the local density approximation (LDA). We report results on the geometry, IP [13], and EA obtained both with frozen-core all-electron calculations [14, 15] and angular-momentum-dependent pseudopotentials [6]. As expected, there is practically no difference. Clearly, for the properties listed, the LDA results seem to be better than HF. Gradient corrections (BLYP [6]) to the exchange and correlation functionals appear to improve the results for the structure and the EA, but to reduce the good agreement for the IPs. There is no fundamental reason to expect that gradient corrections improve the IP. However, the excellent agreement found between the experimental value and the LDA result may in part be fortuitous, because this calculation may well suffer from an incomplete treatment of the multiplet structure of the cation. As the comparison between vertical and adiabatic IP and EA reveals, the effect on the energy that the structural relaxation resulting from the addition of either a hole or an electron to C_{60} has is small. The structural changes, on the other hand, are not negligible. The bond-length values for each type of bond in C_{60} acquire a non-negligible dispersion: for instance, BLYP calculations predict a dispersion of about 0.02 Å in the cation (1.395–1.416 Å; 1.448–1.469 Å), and a slightly smaller one in the anion (1.402–1.416 Å; 1.449–1.465 Å).

Unfortunately, calculations generally ignore zero-point-motion effects. In Ref. [16], the resulting root-mean-square displacement was estimated to be of the same order as the difference of the two bond lengths. It was also shown that this has a significant influence on quantities such as the pair-correlation function that, experimentally, can be derived from neutron scattering data. Thus, the bond separation cannot be directly derived from these experiments, not even at low temperatures (20 K).

Table 2 shows analogous results for C_{70}, for which also several calculations are available [17-19]. Comparison of HF, LDA and BLYP can be made along the same lines as for C_{60}. The type of change these methods predict relative to it and the trend in passing from the polar to the equatorial region are similar. In particular, the bonds in the poles that constitute the C_{60}-like portion of the structure are, within less than 0.01 Å, the same as in C_{60}, and the longest bonds belong to the hexagon–hexagon fusions at the equator. Unfortunately, the comparison with measured values is not straightforward because of a basic difficulty to assess the molecular structure from experiments [20]. Data were obtained using diffraction of X-rays (XRD) in $C_{70}6S_8$ solids [21-23], electrons in both the gas (GED) [20] and solid (SED) phases [24], and neutrons [25]. Also NMR and the sensitivity of calculated chemical shifts to the structure have been invoked to help solve this issue [20]. The most striking observation in electron diffraction is the unexpected length of the equatorial bond: 1.538 Å, a value almost identical to that of the C–C bonds in diamond. The only reasonable explanation for this is the effect of thermally excited vibrations, whose amplitude is relatively high for these atoms. Furthermore, as in C_{60}, zero-point-motion effects cannot be neglected in C_{70} either, as shown in Ref. [26]. Their influence can clearly and directly be seen when comparing calculated pair correlation functions to radial distribution functions extracted from neutron scattering data [25], as shown in Fig. 2. In particular, the resulting mean-square displacement of the atoms is estimated to be 0.07 Å [26]. Regarding the results for both IP and EA and their comparison with experiment [27, 28], the same comments as for C_{60} can be made.

Vibrational frequencies are reported in Table 3 for C_{60}: They refer to optically active modes, for which a number of experimental data are available [2a]. We have already commented on the results of the HF method. Regarding DFT calculations, only values obtained with highly convergent pseudopotential calculations are listed [6]. Indeed, several LDA calculations have been published (see e.g. [16, 26, 29-32]) that suffer mainly from limitations in the wavefunction basis sets [33]. This restriction is responsible for significant changes in the structure, and especially in the vibrational frequencies. The difficulty encountered in calculating vibrational spectra accurately is apparent and well-known to the practitioners. Yet, at least in the literature on fullerenes, it has too rarely been emphasized.

The comparison of LDA and BLYP results in Table 3 nicely reflects the differences found in the bond lengths in the two approaches: being dependent on average structural properties, the frequencies of the mostly radial modes are very close, while those of the modes with predominant tangential character differ sizeably. Similar conclusions can be derived from the results obtained for C_{70} in Table 4 [34].

Whereas the comparison of *ab-initio* results from different methods can be rationalized well, that with the semi-empirical methods (see Ref. [3]) is less direct. Amongst these, calculations based on the quantum-chemical force field for π electrons (QCFF/PI) have been recognized to be the best performant for C_{60}, especially concerning vibrational spectra [35]. Having its origin in HF, also this method tends to harden the tangential modes significantly. For C_{70}, the overall comparison of the QCFF/PI frequencies [36] with, say, the BLYP results is of the same type as for C_{60}, although the discrepancy between the two predicted geometries is more pronounced (bond lengths in the range of 1.398–1.492).

Contrasting the eigenvectors determined *ab-initio* with those obtained by semi-empirical approaches would be more instructive, and an attempt in this direction has recently been made [37]. The discrepancy between these different descriptions should also be reflected in physically significant quantities, such as IR absorption or Raman intensities and the electron–phonon coupling constant [38]. However, there still is a lack of stringent comparisons of this kind.

In contrasting theory to experiment, additional considerations must be made: (i) The calculated frequencies are obtained in the harmonic approximation, whereas the observed spectra contain anharmonicity effects that usually tend to lower the harmonic values. So far, no quantitative estimate of this effect has been given. (ii) Most experimental data refer to condensed phases [39], while most theoretical results refer to the isolated molecule, so that the appropriate comparison is indeed that with gas-phase data [40]. (iii) Regarding experiments in the solid phases, we note that in Ref. [30] LDA calculations for C_{60} [33] are extended to a face-centered-cubic crystal and show that solid-state effects are minor. This is qualitatively correct. However, a quantitative assessment cannot be obtained from LDA solid-state calculations on bare fullerenes, because they are affected by the incorrect LDA treatment of the intermolecular interactions (see below). (iv) Regarding experiments in solutions, the interpretation clearly is not straightforward. The assignment of the observed spectra is often far from trivial. It has been demonstrated [41], for example, that the interaction with the solvents can strongly lower the molecular symmetry, thereby render modes that are optically silent in the gas phase active in solutions, and give rise to strong resonance enhancements. (v) In the case of C_{70}, both Raman and IR spectra measured in solid films are also incomplete. Any assignment from experiments is rendered very difficult by the unfortunate combination of several negative factors: the limited knowledge, the existence of a high energy density in some regions of the spectrum, and the presence of orientational disorder, which relaxes the polarization rules for the Raman active modes.

Other issues

There are several fundamental properties of fullerenes for which theoretical (*ab-initio*) approaches do not yet seem able to provide an appropriate or accurate description. These include many physical properties of the solid phases and the nature of the excited states.

The basic crystal structures of C_{60} (fullerite) are close-packed: face-centered cubic at room temperature, and simple cubic with four molecules per unit cell below $\sim$255 K. The distance of closest approach of the molecular units is about 3.1 Å, a value comparable to the interlayer spacing of carbon sheets in graphite. There is no doubt that van-der-Waals interactions play an important role in the intermolecular binding. In spite of this, LDA calculations of intermolecular distances and bulk modulus are in very good agreement with experiment [42]. In my opinion, this is a puzzle that has generally been overlooked. In fact, in LDA the long-range part of the potential is not correct and van-der-Waals interactions are not accounted for. This flaw of LDA–DFT calculations affects the determination of all properties reflecting the intermolecular interaction, such as the band dispersion of electron and vibrational levels in fullerites, and hampers the determination of, e.g., the preferred crystal structure and the frequencies of the intermolecular vibrations, as well as the study of the transformations C_{60} undergoes as a function of temperature. Classical potentials currently provide the only tool for this study, however, they generally are able to simulate one specific transformation or grasp one specific aspect but not the global phase diagram. Progress in the *ab-initio* description of dispersion forces within the DFT scheme has recently been made [43]. A first step would involve deriving the long-range constants of the van-der-Waals potential from DFT calculations of the multipole polarizabilities, such as done in Ref. [44] for small molecules.

The interest in an accurate description of the excited states of fullerenes [3] and their dynamics is not purely academic [45]. In fact, promising applications of C_{60} and C_{70} exploit the special nature of the lowest-energy triplet states, whose formation via intersystem crossing of excited singlet states is extremely efficient, and of their excitation spectra. In particular, optical absorption in the excited triplet states of both fullerenes is strongly nonlinear, and this is the basis for their use as powerful optical limiters [45]. Another interesting application is for DNA cleavage and photodynamic therapy, which is associated with the fact that photoexcited C_{60} and C_{70}, in the triplet states, generate the highly reactive $^1O_2$ species efficiently [46].

The understanding of the structure of the first excited states is still limited and relies mostly on semi-empirical approaches, which, however, are able to reproduce several features of the optical spectra [3]. For such large molecules, high-level configuration–interaction computations are not yet feasible. On the other hand, excited states constitute a general basic difficulty in calculations based on DFT, although recently a large effort has been made to overcome this limitation at least partially [43, 47]. In this context, a relevant calculation is that of the dynamic hyperpolarizability of the C_{60} molecule using time-dependent DFT [48], which helps establish the origin of the difficulty encountered in determining its value experimentally.

FULLERENE DERIVATIVES

Nowadays a rich variety of fullerene derivatives have been prepared, which are based mostly on C_{60} because of the relatively poor availability of higher fullerenes [49].

The basic and special features of C_{60} chemistry, which are guidelines for functionalization and chemical synthesis, are discussed at length and explained in detail in Ref. [50]. The main property of C_{60}, as was soon recognized, is its high electrophylicity (cf. the high value of the electron affinity in Table 1). This has made it possible to synthesize new compounds via reductive chemical or electrochemical processes, as well as through addition of nucleophiles. In this way, fulleride solids are formed via intercalation of alkali or alkaline-earth metal atoms into the fullerite [51], and also a number of organic molecular complexes are obtained. In particular, the former has given rise to superconductors at relatively high temperatures [38] and the latter, through addition of macromolecular carbanions, to the creation of polymers including the C_{60} moiety (e.g. flagellenes [52]).

Another characteristic of C_{60} is the special reactivity of the "double" bonds. These allow diverse cycloaddition reactions that are at the origin of diverse fullerene functionalizations and polymerization. Owing to the special structure of the carbon cage, a rich multiplicity of structural isomers results: hence the need for controlled functionalization via regioselective reactions. On the other hand, other interesting derivatives, also characteristic of fullerenes, are more difficult to obtain. These consist in the substitution of one or more carbons and in the complexation via atom encapsulation.

Here we shall discuss selected systems that currently attract widespread interest and for which theoretical approaches can provide crucial understanding. The selected issues touch on fundamental aspects of the chemistry and physics of fullerenes. The response to them exemplifies well both successes and limitations of our investigation so far.

C_{60} *polymers and dimers*

The first indication of polymerized fullerenes came from experiments on oxygen-free C_{60} films, which transform when irradiated by either visible or ultraviolet light [53, 54]. Formation of polymers of different dimensionality also accounted for the existence of unusual structures obtained at high-pressure and high-temperature conditions [55, 56]. Nevertheless, the discovery of C_{60} polymers in the low-temperature intercalated phases K_xC_{60} and Rb_xC_{60} with $x = 1$ [57, 58], was, at first, received not without doubts. Soon the evidence confirming such a proposal grew [59], and this became the focus of intensive research activity [60]. In these three cases, the binding of molecular units was described as the result of a [2+2] (cyclo)addition reaction that involves the "double" bonds of the fullerene and gives rise to a characteristic four-membered carbon ring (Fig. 3(a)). C_{60} dimers are quite unusual. Very recently, a C_{120} solid having a "dumb-bell-shaped" ([2+2]) molecular unit as shown in Fig. 3(a) has, however, been synthesized at normal temperature and pressure conditions, using an ingenious chemical treatment [61]. Structural studies of $(K,Rb,Cs)_1C_{60}$ have also revealed dimerized phases that were obtained with fast cooling from room temperature [62]. Here, however, the bond is not of the [2+2] type and does not involve the "double" bonds. The two monomers are singly bonded as shown in Fig. 3(b).

In fullerides, new polymer phases have recently been characterized also at higher alkali concentrations, such as Na_4C_{60} [63] or Na_2RbC_{60} [64]. As in the dimerized phases of the A_1C_{60} compounds, two monomers are singly bonded to each other. Multiple additions result in either 2D or 3D polymers. In photopolymerized C_{60}, structural studies are obviously more complex. The change of intensity of the C1S shake-up satellite in X-ray photoemission spectroscopy (XPS) data has been taken as indicator of the formation of the [2+2] rings [65] and monitored up to saturation. This suggests that at saturation their number per molecule is six. A structure of the 2D rhombohedral type has been proposed, which would also agree with one observed in pressure-induced transformations.

This wealth of results still needs a systematic, basic understanding. Indeed, there is quite a bit of confusion in the approach to these compounds, namely, a tendency to "compare everything with everything else" and neglect the fact that all these "bound" fullerenes (either dimers or polymers of different dimensionality obtained in a variety of condensed phases) have different physical properties and origins. Examples of this are the attempt to explain detailed features of vibrational spectra measured in fullerides with those calculated for isolated neutral dimers [66], the unselective comparison of binding energies estimated for isolated dimers with the formation/activation energies derived from experiments in all these different cases, and the discussion of the NMR chemical shifts.

So far, theoretical work has been very material-specific and fragmentary. *Ab-initio* calculations are mostly restricted to isolated dimers as well as to the calculation of binding energies and structural parameters. Table 5 contains a comparison between different methods for neutral as well as doubly charged dimers [6, 67, 68]. The latter are interesting as models of the fullerene anions of alkali fullerides. Bond lengths are reported only in the neighborhood of the intermolecular bond, where the largest structural modifications occur.

The electronic structures of neutral and doubly charged C_{60} dimers are different, and hence also their structural preferences and energetics. A strong dependence of the energies on the type of approximations used in the calculations is also evident. One source of discrepancy is physical, namely, the approximation used to represent the exchange and correlation energies [69]. Such structures in which the carbon–carbon bonds are highly stressed are difficult to represent accurately. Moreover, formation energies suffer from the failure of both HF and local or semi-local approximations in DFT to represent van-der-Waals interactions. The other source of discrepancy evident in Table 5 is of technical nature and results from the different basis sets used in the calculations. For the localized functions the convergence is poor, while for the plane-wave approach it is well achieved. Despite the quantitative disagreement, some common and clear messages can be deduced from inspection of the results as well as from the comparison with Table 1.

In all cases, the dimer forms with an unusually long bond for carbon–carbon systems, and the bond pattern on the individual molecules is strongly affected. Apart from the [2+2] neutral dimer in LDA and HF, all the calculated energy minima in Table 5 correspond to metastable states. Note that the bond orders [4] calculated within the BLYP–DFT scheme for the "square" are 0.88 for the intramolecular and 0.90 for the intermolecular bond. For the singly bonded neutral dimer, none of the quoted calculations found a minimum. For the C_{60} dianion, DFT with gradient-corrected functionals predicts a singly bonded isomer with anti-conformation as ground state [70], while LDA would slightly favor the [2+2] configuration. In all cases, the charged dimer is unstable.

How and to what extent can we compare these findings with experimental data? For the formation energies, there are no unambiguous experimental data. What seems to be established is that in the solid, [2+2] dimers dissociate upon heating at 175 °C. As mentioned above, even considering the best-converged calculations, it is intrinsically impossible to predict the formation energy for such a structure with an accuracy of better than $\sim$10 kcal/mol. It is quite clear, however, that interdimer interactions in the solid are crucial to its stabilization. On the other hand, Coulomb repulsion clearly disfavors the stabilization of dianions even further. This requires the presence of counterions, as in the dimeric quenched phases of alkali-metal fullerides.

The use of simple standard chemical pictures and standard or incorrect terminology has also helped confound the description of these unconventional bonding situations. For instance, the intermolecular bond in the singly bonded dimer has been referred to as "single" bond and contrasted to those in the [2+2] isomer, where, as we have seen, not double bonds but two, also long and weak bonds exist. The quaternary carbon has often been classified as sp^3 in both types of structures, although its geometrical and electronic environment is not only different from that of an sp^3 carbon but also from one situation to the other. Indeed, the measured values of the chemical shift for the bridging carbons estimated from ^{13}C MAS–NMR are 78 ppm for the dimeric phase of Rb_1C_{60} [71], but 35 and $\approx$45 ppm for the [2+2] polymeric phase of Rb_1C_{60} [72] and K_1C_{60} [73], respectively. Moreover, in the 2D polymerized high-pressure phase, measurements of the same type give 74 ppm [74], and for the C_{120} [2+2] molecular solid, the value from NMR in solution is 76 ppm [61]. This scenario is not as simple and certainly deserves a thorough theoretical investigation as well.

Figures 4(a) and 4(b) illustrate a representative isodensity hypersurface of the HOMO in both isomers of the charged dimer. It is evident that in the singly bonded configuration the HOMO is a bonding state, while in the [2+2] geometry it is not. Also, in the former the amplitude is large in the neighborhood of the intermolecular bond, and particularly on the carbons at the α positions. This is definitely not the case in the latter. For a further discussion of the electronic structure of the singly bonded dimers, the reader is referred to the section on heterofullerenes, where the comparison with the isoelectronic diazafullerene is made [75, 76].

Besides a characterization of the chemical and dynamical properties of these species, progress in this field will also require that the microscopic mechanisms driving either dimer or polymer formation be unraveled. In the case of photopolymerized C_{60}, there are indications that the transformation proceeds via the triplet state [54]. A more complete understanding should eventually help in finding a way to control polymerization, namely its initiation and its propagation in one-dimensional chains or structures of higher dimensionality.

Heterofullerenes

Heterofullerenes is a general name given to derivatives that originate by substitution of carbons on the shell, and that retain the characteristic structural properties of the parent molecules to a large extent. Indication that such unusual molecules exist originally came from mass spectra of a few boron-"doped" carbon clusters in the size range of fullerenes [77]. Calculations of diverse levels that tried to identify specific physical and chemical properties induced by the substitution soon followed [78, 79].

So far, successful production beyond the realm of cluster beams is limited to "azafullerenes", which are derived by nitrogen substitution [80]. Electronically, replacing one carbon on the shell with nitrogen in $C_{59}N$ corresponds to adding one electron to the π-system of C_{60}. In principle, this could provide a unique way to explore the properties of "modified" C_{60} anions, which could be relevant for the investigation of superconducting and ferromagnetic behavior of C_{60} compounds (see e.g. [81]), and eventually for the generation of new phases exhibiting such properties. However, the modification induced by nitrogen and the localization effects due to the excess core charge were not trivial, and gave rise to specific reactions and unexpected compounds.

In fact, $C_{59}N$ [78] is a radical, with an unpaired electron mostly localized on the carbon atom (C′) closest to the nitrogen (see Figs. 5(a) and 6(a)). Hence, it readily reacts to form closed-shell molecules in which C′ becomes four-fold coordinated: the hydrogenated monomer $C_{59}HN$ [82] (Fig. 5(b)) and the dimer $(C_{59}N)_2$ [80] (Fig. 5(c)). The latter is a rather unique derivative: It is the only dimer currently known to be highly stable both in solution and in the solid phase [83].

In order to elucidate the basics of these new species and understand whether they "teach us" something new about fullerene chemistry, some key questions must be dealt with: How and to what extent does nitrogen substitution alter the properties of the parent molecule? What is the mechanism that stabilizes $(C_{59}N)_2$ compared to the dianion? BLYP–DFT calculations [68] have helped finding the answer by determining the structures [83] and by characterizing the electronic behavior in detail [84, 85]. The structure of the ground state of $C_{59}HN$ has C_s symmetry (Fig. 5(b)) and that of $(C_{59}N)_2$ has C_{2h} symmetry, with the nitrogens in a trans configuration (Fig. 5(c)). Table 6 contains calculated values for the structural and electronic characteristics, which, when contrasted with those in Tables 1 and 5, elucidate some of the substitution effects. Compared to C_{60}, only confined modifications occur in the bond lengths in $C_{59}N$: primarily C′–N is elongated compared to the "double" bond in C_{60}, and the "single" bonds shrink. The changes are strongly enhanced in $C_{59}HN$, where C′ is saturated by hydrogen, which strongly weakens all other bonds. Interestingly, the structural changes induced on the shell strongly resemble those due to dimerization. The structure of the dimer is quite similar to that of the singly bonded C_{120}^{2-} (Table 5), but the C′–C′ intermolecular bond is about 0.07 Å shorter. The calculated bond order [4] is about 0.77 in the former and 0.70 in the latter.

As mentioned in Ref. [68], the distribution of the spin density in $C_{59}N$ strongly resembles that of monoalkyl radical adducts [86], which also form dimers in solutions. However, apparently in these cases the direct C′–C′ link does not realize owing to steric effects, so that the final configuration is different.

Significant electronic differences exist between the two azafullerenes. This is reflected for instance in the redox properties, the optical response, and the NMR data. Note that the IP of the dimer is much lower (~ 0.8 eV) than that of C_{60}, while the EA is ~ 0.3 eV higher (see Table 6). The values in $C_{59}HN$ resemble more those of a C_{60} doubly charged anion.

Similarly to the case of the dimeric and polymerized unsubstituted phases discussed above, care must be taken in describing these unconventional bonding situations. Again, the quaternary carbon C′ has often been classified as sp^3 in the azafullerenes [87, 88]. However, as pointed out in Ref. [68], examining the electron density distribution (Fig. 6(b)) revealed that the electronic environment of C′ was "remarkably different from that of a typical sp^3 atom" (in terms of both spatial distribution and isotropy) in the dimer, while in the hydrogenated monomer (Fig. 6(d)) it was closer to that of a conventional sp^3 carbon. Subsequently, the calculation of the chemical shifts was able to confirm and explain this picture better. These values [85] turned out to be in good agreement with measured ^{13}C resonances of NMR: 90.3 (theory: 85) ppm in the dimer, and 72.1 (theory: 68) ppm in $C_{59}HN$. The former is indeed intermediate between the characteristic range of chemical shifts pertaining to aliphatic and olefinic (or aromatic) carbon atoms [89], whereas the latter pertains to a saturated carbon and is thus closer to the aliphatic side [90]. The localization properties of the excess electrons have recently been studied using a combination of experiment (photoemission) and theory [84].

As $(C_{59}N)_2$ is isoelectronic with a hypothetical dimer of the C_{60} anion, calculations can easily characterize similarities and differences and thus extract the peculiarities of heterodoping with respect to mere electron donation. Despite the great similarity of the structures, a crucial discrepancy is reflected in the energy involved in the intermolecular bonding. $(C_{59}N)_2$ is bound with respect to the isolated monomers by 15 kcal/mol, whereas $(C_{60}^-)_2$ is disfavored with respect to dissociation by 47 kcal/mol. This accounts for the fact that the latter are not stable unless counterions are present, as in the quenched dimeric phases of alkali fullerides A_1C_{60} [62], while the former is stable. The electron density distribution of the HOMO in $(C_{59}N)_2$ (Fig. 6(c)) is of particular interest: It is almost a mirror of the HOMO of the C_{120}^{2-} in Fig. 4(b), as it is mainly concentrated on the N atoms and along the axis of the intermolecular bond. This similarity also extends to the low-energy manifold of the unoccupied states.

The availability of solids of A_1C_{60} and of the diazafullerene provides a better opportunity to investigate and compare their properties experimentally. Combining XRD, NMR, photoemission, electron energy-loss spectroscopy, and theory has in fact provided further insight. The crystal structures of the dimeric fullerides and that of diazafullerene are very similar [62, 83], and the molecular units are confirmed to have the calculated configurations.

Interesting features emerge in the electronic properties. We recall that in the dimeric phase of Rb_1C_{60}, the measured value of the chemical shift for the bridging carbons is 78 ppm [71]. This is 12 ppm lower than in the diazafullerene, in accordance with the absence of the deshielding effect of the nitrogen atom. In spite of the similarity of the electronic structure just discussed, comparison of the photoemission spectra shows an apparently significant discrepancy between the two systems [75, 84]. While for the heterofullerene the highest peak in the occupied part of the spectrum is unsplit, with a shoulder ascribable to the excess electrons, the photoemission feature at highest energy for Rb_1C_{60} clearly consists of two peaks separated by $\sim$0.3 eV and is split off from the rest of the spectrum by $\sim$1 eV. However, the difference is easily understood and lies in the HOMO and HOMO-1 levels relative to the rest of the spectrum, which, in the heterofullerene, are lowered by the additional positive charge on the nitrogen cores. As a consequence, the forbidden energy gap in $(C_{59}N)_2$ is about 1 eV larger: another manifestation of the stabilization effect of the "on-ball" doping.

Although the production of azafullerenes is certainly not over [91] and our knowledge of their rich chemistry is far from exhaustive, it is natural to extend our imagination and hope to other interesting derivatives that could be obtained by substitution. The discussion above clarifies that nitrogen substitution represents a special case, in that the perturbation it drives on the structure of the carbon fullerene is limited. In this respect, also boron is a promising candidate [78], and a solid phase with tetrahedrally coordinated monomers of $C_{59}B$ has already been reported [92]. However, the stability of such systems and the possibility of mass production are still unclear.

Metallofullerenes

Metallofullerenes is the generic name given to host–guest complexes formed by fullerenes with metal atoms encapsulated [93, 94]. Among the so-called endohedrally doped fullerenes [95], they constitute the most interesting case from the point of view of the design of novel materials. In particular, there is widespread hope that new ferroelectrics or ferromagnetic phases can be obtained from them, but research has long been hampered by the difficulty of isolating and purifying such molecules with the methods commonly used for C_{60}. C_{60} is the most desirable host from both practical and fundamental points of view. However, for a long time — for reasons still largely unclear — it was not possible to isolate metallofullerenes based on it [96]. Only very recently has this been achieved with ion sputtering [97], especially using alkali-metal ions. Higher fullerene-based metal endohedrals, on the other hand, are comparatively easier to obtain, and in some specific cases have recently become available in relatively large quantities [98-100].

In spite of intense experimental work aimed at characterizing these derivatives, several and basic questions are still unanswered. For instance, it is difficult to obtain exhaustive and direct information on the structure of these complexes solely from experiment. Indeed, with the exception of C_{60} and C_{70}, one is faced with the problem of understanding which of the many possible cage isomers are present in a given sample. In the case of diamagnetic systems, such as $Sc_2@C_{84}$ [101] or $Ca@C_{82}$ [100], NMR has provided the desired characterization for some of the isomers. For paramagnetic systems, such as the long-studied $La@C_{82}$, no clue has so far emerged from experiment. Electron-paramagnetic resonance (EPR) experiments, which were vital for the detection of this and similar systems, have often also indicated the presence of more than one isomer [102, 103]. Regarding the position(s) of the guest atom(s) inside the cage, direct information can so far be inferred only from XRD. For $Y@C_{82}$ [99] XRD-derived charge density maps show that the metal atom is off-center.

Thorough theoretical work can indeed assist experiment in figuring out the physical and chemical properties of such complexes. So far, calculations have been restricted to isolated molecules. There are only very few semi-empirical approaches, because of the intrinsic difficulties encountered in modeling metal atoms and their interactions with carbon. Standard *ab-initio* calculations are static, and often use symmetry constraints that would only be appropriate for the specific isomer of the bare fullerene. As such, they are frequently inadequate for the endohedrally doped fullerene, and have strongly biased the way metallofullerenes are generally thought of. Owing to the well-known reduction properties of fullerenes, all the metal atoms considered so far act as electron donors inside the carbon cage and, regardless of the position they occupy, tend to lower the symmetry of the molecule. Moreover, static calculations hamper the investigation of possible motion for the guest atom inside the cage. No wonder that these limitations existed in the early days of fullerene research, when calculations free of symmetry constraints were rarely affordable. Nowadays, however, such restrictions can in principle be overcome. Unfortunately many calculations on high-fullerene endohedral complexes still use symmetry constraints, thus biasing the conclusions (see e.g. [104-107]).

The earliest investigations were on C_{60} with the metal atom kept fixed at the center of the molecule [108, 109]. DFT–LDA calculations using molecular dynamics to search for minimum energy configurations were the first to demonstrate that the energetically favorable positions for the metal atom were off-center [110, 111] and that the center did not even correspond to a minimum of the potential energy surface [112]. Qualitatively, this can be understood at various levels. Acting as an electron donor to the threefold-degenerate t_{1u} states of C_{60}, the metal atom induces a Jahn–Teller splitting that drives it away from the center. If we model the cage as a spherical electronic shell, its polarization will be the off-center driving mechanism, and the distance from the carbon shell will depend on the size and charge of the metal ion [113]. If we now allow for the dishomogeneity of the charge distribution and consider the specific bond pattern of the fullerene, we understand that the electron-rich regions, namely the "double" bonds, will act as the attraction centers for the metal ion [114]. Depending on its charge, size and propensity to form a directional bond with the carbons, the guest atom will position itself more or less away from the center of the pyracylene unit surrounding the double bonds. Owing to the delocalized character of the t_{1u} states, additional effects resulting from the distribution of the excess charge density are minor. In Ref. [115] two specific and distinct cases are considered in detail: La@C_{60} and Li@C_{60}, whose binding with carbon is in general very different. Their $T = 0$ positions inside the cage are shown in Fig. 7, together with the distribution of the spin density. The chemisorption site for La closely corresponds to the center of the pyracylene unit, with a first coordination of six and distances in the range of 2.55–2.64 Å. Lanthanum is strongly ionized and to a first good approximation can be considered in the 3+ charge state. This bonding deforms the cage locally in a sizable manner, with an elongation of the "double"-bond lengths up to 0.07 Å. Lithium has a smaller ionic radius and gives up essentially one electron. Thus, it comes closer to the center of the hexagon, and deforms the cage to a lesser extent. The closest shell is composed of six atoms at distances in the range of 2.16–2.22 Å, and the elongation of the pyracylene double bonds is 0.03 Å. The DFT–BLYP value for the binding energy is $\sim$61 kcal/mol for La and $\sim$44 kcal/mol for Li.

In the case of higher fullerenes, the possibility of many different isomers for the cage itself [116] renders the search more complex. However, similar considerations can be used to figure out which endohedral positions are favorable for metal chemisorption [114, 115]. Which one of all the possible iso- and hetero-cage isomers is energetically the most favorable one will depend on the combined effect of several factors: the relative stability of the neutral carbon cages, their propensity to "receive electrons" relative to the tendency of the metal atom to ionize, the type of binding allowed by a specific geometry, and the distribution of the molecular orbitals that act as acceptors. Excess electrons can either be delocalized over the carbon shell or tend to localize at some specific regions, depending on the structure of the cage. If localized, they will tend to render certain sites more appropriate for metal chemisorption. DFT–BLYP results for C_{82} and La@C_{82} are discussed in Ref. [115]. We report them in Table 7, with a caveat that they are still partial, as in some cages only local optimization procedures were applied. Some clear messages can nevertheless be extracted: (i) There is a dramatic change in the relative stability on passing from the neutral cages to the corresponding endohedral complexes. This was also pointed out, within a different scheme [117], for other metallofullerenes (e.g. Ca@C_{82} [107] or Sc_2C_{84} [106]). There, however, the energy ordering of the endohedrals was considered to reflect that of the corresponding anions, which is only partly true, as clearly exemplified by the C_{2V} cage. Although it does correspond to the triply charged anion that is lowest in energy, the binding energy of La strongly depends on its position (see Table 7), showing that factors other than the "affinity for three electrons" are also important and can become dominant. (ii) While energy differences between heterocage isomers can be of the order of 10 kcal/mol, those between isocage isomers are one order of magnitude smaller.

It is also worth noting that, in ignorance of the cage structure in the complexes, 82:3 is the one commonly assumed in theoretical studies of La@C_{82} and Y@C_{82} [104, 114, 118] and also in the interpretation of experiments of C_{82} metallofullerenes in general (see e.g. [99, 100, 118]). The motivations for this were plausible: 82:3 corresponds to the ground state of the bare fullerene (see Table 7), for which also NMR detects C_2 as the symmetry of the most abundant isomer [119]. The most commonly assumed image of the endohedral, however, is still one with the metal atom positioned on the symmetry axis, a choice dictated originally solely by the limitations of the early calculations. But, as more recent calculations have shown, this configuration is about 13 kcal/mol higher than the ground state, and thus too high to be a probable geometry at room temperature [114]. In conclusion, as C_2 cages are not especially energetically favorable for La@C_{82}, it is likely that the cages in the various experiments conducted so far may very well be different. Whether C_2 or C_{2V} cages, or a mixture of them, occur, will depend on the production mechanism, namely, on both kinetic and energy factors.

Clearly, calculations of this type are important if one wants to establish the nature of the metal–cage binding and its energetics. However, the static view of endohedrally doped fullerenes with the metal atom stuck to some position inside the cage may not be the correct one. *Ab-initio* molecular dynamics simulations carried out at room temperature have demonstrated that this is at least true for La [114]. In C_{60} (Fig. 8(a)), La diffuses very fast at room temperature, tangentially to the carbon shell, and completes one entire round in about one psec. In C_{82}, analogous simulations have been reported only in the 82:3 cage, and reveal a different type of motion that is confined to the region of the minima and characterized by residence times of the order of 0.1 psec (Figs. 8(b)–(d)). These findings suggest a new picture that is useful for the interpretation of experiments. In fact, even experiments such as EPR, which are generally used to obtain information on molecular dynamics, are not adequate in this case. As their time scale is orders of magnitude longer than that of the motion of the metal atom, the latter escapes detection by such probes. For a more detailed and further characterization of the dynamics of the metal atoms, the reader is referred to Ref. [115].

For further progress in the field of metallofullerenes, it would be desirable to obtain insight into the possible effects of the environment on their physical and chemical properties. By environment I mean both the solutions in which most experiments are performed as well as the other molecular units in solid phases. The latter are obviously important from a materials-science point-of-view, because the extent and nature of their correlations will eventually determine the electronic and magnetic properties of the real materials. Research aimed at finding a way to open and close fullerene cages in a controlled fashion [120, 121] could, in principle, benefit from computer simulations and quantum-chemistry calculations. However, key quantities, such as the free energy barriers, are difficult to calculate with the desired accuracy. So far, only rough estimates of $T = 0$ energy barriers have been obtained with static calculations [122].

Other derivatives and issues

I have focussed only on few selected systems in order to present a more critical review. However, I would like to mention some other most relevant derivatives, for which relatively few computations are available, and some general questions.

An extremely interesting derivative is TDAE–C_{60} [81]. It is currently the only one that presents a ferromagnetic phase and has a higher critical temperature (16 K) than any other organic compound. Apparently all efforts to replace TDAE with another electron donor have so far failed to provide magnetic ordering. Its electronic and magnetic behavior is complex and constitutes one of the most intriguing open questions in this field (for recent work, see e.g. [123]).

A still academic, but uncommon and peculiar type of derivatives are metal-coated C_{60}'s, i.e. binary clusters with a C_{60} core decorated by metal atoms. So far they have only been characterized in the gas phase by means of mass spectra [124]. These show rather clear magic numbers when alkali and alkaline-earth metals are used, in agreement with the completion of either a geometrical or an electronic shell [124-126]. Having fullerenes coated with transition metal "layers" would obviously be very interesting. Success has been achieved with Ti, V, Zr and Nb, for which mass spectra reveal characteristic magic numbers, whose origin is still not understood [127]. However, the stability and reactivity properties of all these clusters, which will be decisive for their usefulness in nanostructured materials, are practically unknown.

A recurrent question in the investigation of fullerene compounds concerns the "amount of charge" that is being transferred to the fullerene. To what extent can this question be answered? No individual calculation or experiment can by itself be taken as a quantitative answer. To obtain a good estimate of it, a combination of different data or a comparison with other known systems must be made. Experimentally, neither electronic and vibrational probes nor NMR yield a direct measurement of the charge transfer. Moreover, the changes measured in, e.g., vibrational frequencies [39] or XPS lines from one derivative to the pristine molecule in general result also from other factors and cannot be interpreted solely in terms of charge transfer. Even in the case of complete charge transfer, it has been shown in detail [128] how the shifts in vibrational frequencies also depend on structural relaxation and thus cannot be taken as direct measure of the "donated electrons". Theoretical determination, on the other hand, is often based on the Mulliken population analysis, which becomes inadequate whenever the electron density has delocalized or partially delocalized character. Other repartitions of the charge density can be used (see e.g. [129]), but the final number will depend on the type of repartition itself and on the assumptions made for the reference system. One can nevertheless identify where the excess electrons are mainly "localized" and which Kohn–Sham orbitals become occupied or are mainly modified.

In the case of C_{60}, simple arguments based on the filling of one-electron orbitals (t_{1u} and t_{1g}) suggest that C_{60} can easily accept up to twelve electrons. It has become clear, however, that this limit is difficult to attain. For the moment, it has only been shown to happen in exohedral complexes, namely, the metal-coated $Li_{12}C_{60}$ and $Ca_{32}C_{60}$ [125, 126], where the two bonds of C_{60} become almost identical. In the gas phase and in solution, the electron attachment limit is much lower (two and six [50, 130], respectively). In intercalated compounds, the maximum transferable charge is limited by constraints on the number of atoms that the interstitial regions of a pristine solid can accommodate. Intercalation in superfullerides can either make the host structure unstable or, as shown both experimentally and theoretically, induce the formation of non-C_{60} states acting as traps for the electrons [131].

OUTLOOK

Research on the physical chemistry of fullerenes still has a long way ahead. In spite of the extensive knowledge of carbon systems and of the apparent structural simplicity of these fascinating molecules, it is by now clear they are by no means simple systems. Conventional mind frameworks or computational schemes used in organic chemistry have often proven inadequate. An in-depth understanding and a quantitative description of physical properties and chemical processes are necessary before we will be able to tailor the properties of fullerenes by functionalization or doping. The aid, which computational approaches can in principle give, is certainly substantial, as is true in any other material-oriented research, provided however that key issues are identified and that the merits as well as the limitations of the adopted methods are well established. The sections above are meant to contribute to this effort.

In each section, I have indicated open issues, the solution of which, in my opinion, would provide the necessary step forward in that particular field. Here, I would nevertheless like to conclude on the one hand by pointing out the strong need for *ab-initio* studies of chemical reactions of fullerenes, especially in condensed phases, and, on the other hand, by expressing my wish to see new directions for the computational approaches develop. In particular, fullerene molecules are bound to have important applications as units of composite optoelectronic devices [45, 132], in nanotechnology [133, 134] and in biology [135, 136]. Progress has recently been made on the experimental side. Unfortunately, reliable computational methods with established predictive power have never been used in conjunction with this activity. I hope that this review has brought convincing arguments that indeed the time is ripe for this challenging effort to be undertaken.

Acknowledgment

I wish to thank Alessandro Curioni for useful discussions and Charlotte Bolliger for her patient and careful editing of the manuscript.

References

[1] The discovery papers are: Kroto HW, Heath JR, O'Brien SC, Curl RF, Smalley RE. 1985. *Nature* 318:162-63, and Krätschmer W, Lamb LD, Fostiropoulos K, Huffman DR. 1990. *Nature* 347:354-58

[2] Interesting books are (a) Dresselhaus MS, Dresselhaus G, Eklund PC. 1996. *Science of Fullerenes and Carbon Nanotubes* San Diego: Academic Press, Inc.; (b) Andreoni W, ed. 1996. *The Chemical Physics of Fullerenes 10 (and 5) Years Later*, NATO ASI Series E: Applied Sciences, Vol. **316**, Dordrecht: Kluwer; (c) *Proc. 11th Int'l Winterschool on Electronic Properties of Novel Materials: Molecular Nanostructures, Kirchberg, Austria, March 1997.* Singapore: World Scientific. In press

[3] Cioslowski J. 1995. *Electronic Structure Calculations on Fullerenes and Their Derivatives.* New York: Oxford University Press

[4] Bond orders are calculated from Mulliken population in a localized functions scheme. Owing to the general incompleteness of the basis functions in which the electron wavefunctions are expanded, the values thus obtained must be considered only estimates. However, when a good degree of convergence is reached in both cases, the values obtained for a derivative are meaningful if compared to those in C_{60}

[5] A rather exhaustive review (up to 1994) is contained in Ref. [3]. It is detailed in accounting for Hartree–Fock and post-Hartree–Fock calculations but does not mention the specific computational scheme used in the various "LDA" calculations. This inevitably creates confusion. Clearly, also LDA calculations should be "evaluated" according to the specific computational scheme, e.g., the wavefunction basis sets used

[6] All the results reported in Tables 1–7 for P-LDA and P-BLYP use the same scheme so as to provide a framework for meaningful comparisons. Electronic wavefunctions are expanded in plane waves up to an energy cutoff of 55 Ry, and pseudopotentials (P) constructed from all-electron calculations with the Troullier–Martins procedure (Troullier N, Martins JL. 1991. *Phys. Rev. B* 43:1993-2006). In all cases of open-shell configurations, spin-polarized functionals have

been considered. Calculations on isolated molecules use the procedure introduced by Barnett and Landman (Barnett RN, Landman U. 1993. *Phys. Rev. B* 48:2081-97). Previous reports of results obtained with such a scheme in either local-density (LDA) or gradient-corrected (BLYP) approximations for C_{60} and derivatives can be found in [68], [84], [115], and [129]. Original references to BLYP are the following papers: Becke AD. 1988. *Phys. Rev. A* 38:3098-100; Lee C, Yang W, Parr RG. 1988. *Phys. Rev. B* 37:785-89. Vibrational frequencies were obtained with finite difference calculations of second derivatives. The code used for all these calculations is CPMD in the 2.5 version (Copyright by IBM Corporation) developed by J. Hutter

[7] Scuseria GE. 1991. *Chem. Phys. Lett.* 176:423-27

[8] Hedberg K, Hedberg L, Bethune DS, Brown CA, Dorn HC, Johnson RD, deVries M. 1991. *Science* 254:410-12

[9] A simple, early description can be found in Schlüter M, Lannoo M, Needels M, Baraff G.A, Tománek D. 1992. *J. Chem. Phys. Solids* 53:1473-85; see also Ref. [2a], Chapter 11

[10] Haeser M, Almloef J, Scuseria GE. 1991. *Chem. Phys. Lett.* 181:497-500

[11] see Ref. [3], p. 57

[12] (a) Dreizler RM, Gross EKU. 1990. *Density-Functional-Theory.* Berlin: Springer-Verlag (b) Parr RG, Yang W. 1989. *Density-Functional Theory of Atoms and Molecules.* New York: Oxford Science Publications

[13] Note that some LDA calculations report only the position of the HOMO, which is a very bad approximation, owing to the inaccuracy of the long-range part of the potential

[14] van Wuellen C. 1994. *Chem. Phys. Lett.* 219:8-14

[15] Dunlap BI, Brenner DW, Mintmire JW, Mowrey RC, White CT 1991. *J. Chem. Phys.* 95:8737-41

[16] Kohanoff J, Andreoni W, Parrinello M. 1992. *Phys. Rev. B* 46:4371-73

[17] Scuseria G. 1991. *Chem. Phys. Lett.* 180:451-56

[18] Raghavachari K, Rohlfing CM. 1991. *J. Phys. Chem.* 95:5768-73

[19] Andreoni W, Gygi F, Parrinello M. 1992, *Chem. Phys. Lett.* 189:241-44

[20] Hedberg K, Hedberg L, Buehl M, Bethune DS, Brown CA, Johnson RD. 1997. *J. Am. Chem. Soc.* 119:5314-20

[21] Roth G, Adelmann P. 1992. *J. Phys. I (France)* 2:1541-48

[22] Buergi HB, Venugopalau P, Schwarzenbach D, Diederich F, Thielgen C. 1993. *Helv. Chim. Acta* 76:2155-59

[23] Structural data on C_{70} monoadducts and a further discussion of unsubstituted C_{70} can be found in Seiler P, Herrmann A, Diederich F. 1995. *Helv. Chim. Acta* 78:344-54

[24] McKenzie DR, Davis CA, Cockayne DJH, Muller DA, Vassallo AM. 1992. *Nature* 355:622-24

[25] Nikolaev AV, Dennis TJS, Prassides K, Soper AK. 1994. *Chem. Phys. Lett.* 223:143-48

[26] Onida G, Andreoni W, Kohanoff J, Parrinello M. 1994. *Chem. Phys. Lett.* 219:1-7

[27] Zimmerman JA, Eyler JR, Bach SBH, McElvany SW. 1991. *J. Chem Phys.* 94:3556-62

[28] Bach SBH, Bruce JE, Ramanathan R, Watson CH, Zimmerman JA, Eyler JR. 1993. *On Clusters and Clustering, from Atoms to Fractals*, ed. PJ Reynolds. p. 59. New York: Elsevier

[29] Quong AA, Pederson MR, Feldman JL 1993. *Solid State Commun.* 87:535-39.

[30] Giannozzi P, Baroni S. 1994. *J. Chem. Phys.* 100:8537-39

[31] Adams GB, Page JB, Sankey OF, Sinha K, Menendez J, Huffman, DR. 1994. *Phys. Rev. B* 44:4052-55

[32] Bohnen K-P, Heid R, Ho K-M, Chan CT. 1995. *Phys. Rev. B* 51:5805-13

[33] (i) LDA calculations in Refs. [16] and [26] use an energy cutoff of 35 Ry. This is not fully converged, but fortuitously gives results very close to those of the more accurate and better convergent BLYP calculations. The reason for this is an artifact, but can be easily understood: BLYP yields longer bond lengths than LDA, if treated at the same level of convergence; the same effect is obtained in LDA with a lower energy cutoff, because the short-range attractive part of the core–valence interaction is not fully accounted for. Note also that, at variance with usual calculations based on finite difference computations of the second derivatives, harmonic frequencies in these two references are obtained from LDA–MD trajectories projected onto the irreducible representations of the I_h or D_{5h} symmetry groups. To avoid confusion, we stress that also the correct values obtained in this way for C_{60} are listed in Ref. [26]. There, we explain the mistake made in Ref. [16], where the frequencies were not properly rescaled for the fictitious electron mass of the Car–Parrinello Lagrangian.
(ii) AE–LDA calculations in Ref. [29] use a small basis set consisting of 5s and 4p contracted atom-centered Gaussians. The numerical procedure is explained in detail.
(iii) P-LDA calculations in Ref. [30] use fcc periodic boundary conditions and an energy cutoff of 45 Ry for the plane-wave expansion, which still does not yield converged values for the structural parameters. Here harmonic frequencies are obtained from diagonalization of the dynamical matrix, calculated within the linear response theory.
(iv) LDA calculations in Ref. [31] use a poor basis set for the localized wavefunctions. The details of the numerical methods are not given.
(v) P-LDA calculations in Ref. [32] use fcc periodic boundary conditions and a mixed basis set consisting of one s and three p atom-localized functions and plane waves up to a cutoff of 12 Ry. Frozen-phonon calculations are performed and also diagonalization of the dynamical matrix

[34] A. Curioni and W. Andreoni. In preparation

[35] Negri F, Orlandi G, Zerbetto M. 1992. *Chem. Phys. Lett.* 190:174-78

[36] Negri F, Orlandi G, Zerbetto M. 1991. *J. Am. Chem. Soc.* 113:6037-40

[37] Heid R, Pintschovius L, Godard JM. 1997. *Phys. Rev. B* 56:5925-36. This work compares the results of Ref. [32] and of force-field calculations (Jishi RA, Mirie RM, Dresselhaus MS. 1992. *Phys. Rev. B* 45:13685-89

[38] Gunnarsson O. 1997. *Rev. Mod. Phys.* 69:575-606

[39] Kuzmany H, Matus M, Burger B, Winter J. 1994. *Adv. Mater.* 6:731-45

[40] Frum CI, Engelman Jr R, Hedderich HC, Bernath PF, Lamb LD, Huffman DR. 1991. *Chem. Phys. Lett.* 176:504-8

[41] Gallagher SH, Armstrong RS, Bolskar RD, Lay PA, Reed CA. 1997. *J. Mol. Struct.* 407:81-3. This work also criticizes previous assignments in solutions for C_{60} and C_{70} by Brockner W, Menzel F. 1996. *J. Mol. Struct.* 378:147-63, and in solid films of C_{70} by Jishi RA, Mirie RM, Dresselhaus MS, Dresselhaus G, Eklund PC. 1993. *Phys. Rev. B* 48:5634-42

[42] Troullier N, Martins JL. 1992. *Phys. Rev. B* 46:1754-65

[43] Gross EKU, Dobson JF, Petersilka M. 1996. In: Ed. RF Nalewajski, *Density Functional Theory, Topics in Current Chemistry*, Vol. 181, pp. 81-172. Heidelberg: Springer

[44] Osinga VP, van Gisbergen SJA, Baerends EJ. 1997. *J. Chem. Phys.* 106:5091-101

[45] see Ref. [2a], chapters 13 and 20

[46] see e.g., Foote CS. 1994. *Topics Curr. Chem.* 160:347

[47] Bauernschmitt R, Ahlrichs R. 1996. *Chem. Phys. Lett.* 256:454-64; Bauernschmitt R, Häser M, Treutler O, Ahlrichs R. 1997. *Chem. Phys. Lett.* 264:573-78

[48] van Gisbergen SAJ, Snijders JG, Baerends EJ. 1997. *Phys. Rev. Lett.* 78:3097-100

[49] Recent progress in the synthesis of derivatives of higher fullerenes is reported in Thielgen C, Herrmann A, Diederich F. 1997. *Angew. Chem.* 36:2268-80

[50] Hirsch A. 1994. *The Chemistry of the Fullerenes.* Stuttgart, Germany: Georg Thieme Verlag

[51] for a review, see Fischer JE, in Ref. [2b], pp. 359-82

[52] Samulki ET, DeSimone JM, Hunt Jr MO, Meuceloglu YZ, Jarnagiu RC, York CA, Labat KB, Wang H. 1992. *Chem. Mater.* 4:1153-57

[53] Rao AM, Zhou P, Wang K-A, Hager GT, Holden JM, Wang Y, Lee WT, Bi XX, Eklund PC, Cornett DS, Duncan MA, Amster IJ. 1993. *Science* 259:955-57

[54] Zhou P, Dong ZH, Raol AM, Eklund PC. 1993. *Chem. Phys. Lett.* 211:337-40; Wang Y, Holden JM, Domg ZH, Bi XX, Eklund PC. 1993. *Chem. Phys. Lett.* 211:341-45; Cornett DS, Amster IJ, Duncan MA, Rao AM, Eklund PC. 1993. *J. Phys. Chem.* 97:5036-39

[55] Nunez-Regueiro M, Marques L, Hodeau J-L, Bethoux O, Perroux M. 1995. *Phys. Rev. Lett.* 74:278-81

[56] Isawa Y, Arima T, Fleming RM, Siegrist T, Zhou O, Haddon RC, Rothberg LJ, Lyons KB, Carter Jr HL, Hebard AF, Tycko R, Dabbagh G, Krajewski JJ, Thomas GA, Yagi T. 1994. *Science* 264:1570-72

[57] Chauvet O, Oszlányi G, Forró L, Stephens PW, Tegze M, Faigel G, Jánossy A. 1994. *Phys. Rev. Lett.* 72:2721-24

[58] Stephens PW, Bortel G, Faigel G, Tegze M, Jánossy A, Pekker S, Oszlányi G, Forró L. 1994. *Nature* 370:636-39

[59] For a review, see Chauvet O, Forró L., in Ref. [2b], pp. 383-401

[60] See the entire issue No. 3 of *Applied Physics A*, Vol. 64 (1997)

[61] Wang G-W, Komatsu K, Murata Y, Shiro M. 1997. *Nature* 387:583-86

[62] Zhou Q, Cox DE, Fischer JE. 1995. *Phys. Rev. B* 51:3966-69; Oszlányi G, Bortel G, Faigel G, Granasy L, Pekker S, Stephens PW, Bendele G, Dinnebier R, Mihaly G, Janossy A, Chauvet O, Forró L. 1995. *Phys. Rev. B* 51:12228-32

[63] Oszlanýi G, Baumgartner G, Feiger G, Forró L. 1997. *Phys. Rev. Lett.* 78:4438-41

[64] Prassides K, Vavekis K, Kordatos K, Tanigaki K, Bendele GM, Stephens PW. 1997. *J. Am. Chem. Soc.* 119:834-35

[65] Onoe J, Takeuchi K. 1997. *Phys. Rev. Lett.* 79:2987-89

[66] Porezag D, Pederson MR, Frauenheim T, Koehler TK. 1995. *Phys. Rev. B* 52:14963-70. Most of the calculations are made within the LDA–tight-binding scheme. For the structure thus optimized for the [2+2] dimer, binding energies are also calculated using a Gaussian basis set (same method as in Ref. [29]) in the AE–LDA and AE–GGA with Perdew–Wang functionals (Perdew JP, Wang Y. 1992. *Phys. Rev. B* 45:13244-49).

[67] Scuseria G. 1996. *Chem. Phys. Lett.* 257:583-86

[68] Andreoni W, Curioni A, Holczer K, Prassides K, Keshavarz-K. M, Hummelen JC, Wudl F. 1996. *J. Am. Chem. Soc.* 118:11335-36

[69] For the B3P and B3LYP approximation of the exchange-correlation functionals see: Becke AD. 1993. *J. Chem. Phys.* 98:5648-52

[70] Note that earlier semi-empirical calculations also predicted this molecular conformation. Kürti J, Németh K. 1996. *Chem. Phys. Lett.* 256:119-25

[71] Thier K-F, Mehring M, Rachdi F. 1997. *Phys. Rev. B* 55:124-26

[72] (a) Alloul H, Brouet V, Forró L. 1996. *Phys. Rev. Lett.* 76:2922-25; (b) Thier KF, Zimmer G, Mehring M, Rachdi F. 1996. *Phys. Rev. B* 53:496-99

[73] Kaelber T, Zimmer G, Mehring M. 1995. *Phys. Rev. B* 51:16471-73

[74] Goze C, Rachdi F, Hajji L, Nunez-Rigueiro M, Marques L, Hodeau JL, Mehring M. 1996. *Phys. Rev. B* 54:3676-78

[75] Poirier DM, Olson JH, Weaver JH. 1995. *Phys. Rev. B* 52:11662-64

[76] For calculations of electronic and magnetic properties of the solid fullerides see Erwin SC, Krishna GV, Mele EJ. 1995. *Phys. Rev. B* 51:7345-48; Mele EJ, Krishna GV, Erwin SC. 1995. *Phys. Rev. B* 52:12493-96

[77] Guo T, Jin C, Smalley RE. 1991. *J. Phys. Chem.* 95:4948-54

[78] Andreoni W, Gygi F, Parrinello M. 1992. *Chem. Phys. Lett.* 190:159-63

[79] Kurita N, Kobayashi K, Kumahora H, Tago K, Ozawa K. 1992. *Chem. Phys. Lett.* 198:95-9; Kurita N, Kobayashi K, Kumahora H, Tago K. 1993. *Phys. Rev. B* 48:4850-54

[80] Hummelen, JC, Knight B, Pavlovich J, Gonzales R, Wudl F. 1995. *Science* 269:1554-56

[81] Allemand PM, Khemani KC, Koch A, Wudl F, Holczer K, Donovan S, Gruner G, Thomson JD. 1991. *Science* 253:301-03

[82] Keshavarz-K. M, Gonzales R, Hicks RG, Srdanov G, Srdanov VI, Collins TG, Hummelen JC, Bellavia-Lund C, Pavlovich J, Wudl F, Holczer K. 1996. *Nature* 383:147-50

[83] Brown CM, Cristofolini L, Kordatos K, Prassides K, Bellavia C, Gonzáles R, Keshavarz-K. M, Wudl F, Cheethan AK, Zhang JP, Andreoni W, Curioni A, Fitch AN, Pattison P. 1996. *Chem. Mat.* 8:2548-50

[84] Pichler T, Knupfer M, Golden MS, Haffner St, Friedlein R, Fink J, Andreoni W, Curioni A, Keshavarz-K. M, Bellavia-Lund Ch, Sastre A, Hummelen J-C, Wudl F. 1997. *Phys. Rev. Lett.* 78:4249-52

[85] Bühl M, Curioni A, Andreoni W. 1997. *Chem. Phys. Lett.* 274:231-34. These calculations use the BLYP geometry of Ref. [68]

[86] Morton JR, Preston KF, Krusic PJ, Hill SA, Wasserman E. 1992. *J. Am. Chem. Soc.* 114:5454-55 Morton JR, Preston KF, Krusic PJ, Wasserman E. 1992. *J. Chem. Soc. Perk. Trans.* 2:1425

[87] Bellavia-Lund C, Keshavarz-K. M, Wudl, F. 1997. *J. Am. Chem. Soc.* 119:8101-2

[88] Rachdi F, Hajji, Dolt H, Ribet M, Yildirim T, Fischer JE, Goze C, Mehring M, Hirsch A, Nuber B. 1998. *Carbon.* In press

[89] Lide DR. 1995. *CRC Handbook of Chemistry and Physics*, pp. 9-88. Cleveland: CRC Press. 75th ed

[90] For the measurement and interpretation of the rest of the ^{13}C NMR spectrum, the reader is referred to Refs. [85, 87] and to the paper by Curioni A, Andreoni W, in Ref. [2c]

[91] Nuber B, Hirsch A. 1996. *Chem. Comm.* 12:1421-22; Bellavia-Lund C, Wudl F. 1997. *J. Am. Chem. Soc.* 119:9937-38

[92] Muhr H-J, Nesper R, Kotz R. 1996. *Chem. Phys. Lett.* 249:399-403

[93] Bethune DS, Johnson RD, Salem JR, de Vries MS, Yannoni CS. 1993. *Nature* 366:123-28

[94] A series of review papers on metallofullerenes will appear in the February '98 issue of Appl. Phys. A

[95] In Ref. [3], Chapter 8, a difference is made between endohedral compounds and endohedral complexes, depending on whether host–donor orbital mixing is present

[96] The difficulty refers to extraction and isolation from the soot with HPLC. There is only one report of a successful efficient extraction of several C_{60} metallofullerenes using aniline as solvent: Kubozono Y, Maeda H, Takabayashi Y, Hirakoa K, Nakai T, Kashino S, Emura S, Ukita S, Sogabe T. 1996. *J. Am. Chem. Soc.* 118:6998-99

[97] Tellgmann R, Krawez N, Lin S-H, Hertel IV, Campbell EEB. 1996. *Nature* 382:407-8; Gromov A, Kraetschmer W, Krawez N, Tellgmann R, Campbell EEB. 1997. *Chem. Comm.* 20:2003-4

[98] Kikuchi K, Suzuki S, Nakao Y, Nakahara N, Wakabayashi T, Shiromaru H, Saito K, Ikemoto I, Achiba Y. 1993. *Chem. Phys. Lett.* 216:67-71

[99] Takata M, Umeda B, Nishibori E, Sakata M, Saito Y, Ohno M, Shinohara H. 1995. *Nature* 377:46-8

[100] Xu Z, Nakane T, Shinohara H. 1996. *J. Am. Chem. Soc.* 188:11309-11

[101] Yamamoto E, Tausho M, Tomiyama T, Shinohara H, Kawahara H, Kobayashi Y. 1996. *J. Am. Chem. Soc.* 118:2293-94

[102] Ruebsam M, Plueschau M, Schwitzer P, Dinse K-P, Fuchs D, Rietschel H, Michel RH, Benz M, Kappes MM. 1995. *Chem. Phys. Lett.* 240:615-21

[103] Okabe N, Ohba Y, Suzuki S, Kawata S, Kikuchi K, Achiba Y, Iwaizumi M. 1995. *Chem. Phys. Lett.* 235:564-69

[104] Nagase S, Kobayashi K, Kato T, Achiba Y. 1993. *Chem. Phys. Lett.* 201:475-80

[105] Kobayashi K, Nagase S. 1996. *Chem. Phys. Lett.* 262:227-32

[106] Nagase S, Kobayashi K. 1997. *Chem. Phys. Lett.* 276:55-61

[107] Kobayashi K, Nagase S. 1996. *Chem. Phys. Lett.* 274:226-30

[108] Chang AHH, Ermler WC, Pitzer RM. 1991. *J. Chem. Phys.* 94:5004-10

[109] Rosen A, Wastberg B. 1988. *J. Am. Chem. Soc.* 110:8701-2; Rosen A, Wastberg B. 1989. *Z. Phys. D* 12:387-90

[110] Laasonen KE, Andreoni W, Parrinello M. 1992. *Science* 258:1916-18

[111] Andreoni W, Curioni A. 1994. In *Progress in Fullerene Research*, ed. H Kuzmany, J Fink, M Mehring, S Roth, pp. 93-101. Singapore: World Scientific Publishers

[112] If there is a strong metal–cage bond, such as in La and Y, the energy gained in moving close to the carbons is of a few eV, and corresponds to a change in the charge state of the metal atom

[113] Erwin, SC. 1993. In *Buckminsterfullerenes*, ed. WE Billups, MA Ciufolini, pp. 217-255. New York: VCH Publishers

[114] Andreoni W, Curioni A. 1996. *Phys. Rev. Lett.* 77:834-37

[115] Andreoni W, Curioni A. 1998. In Ref. [94]

[116] Fowler PW, Manolopoulos DE. 1995. *An Atlas of Fullerenes.* Oxford: Clarendon Press

[117] These calculations use a kind of "hybrid" approach. Structural optimization is made at the level of HF. DFT calculations are performed only as single point on the HF geometries using B3P and B3LYP exchange-correlation functionals [69]. The validity of such a procedure is debatable, and certainly the results are inconclusive. In fact, the structural changes the DFT calculations would predict are nonnegligible and involve energy changes of the same order as those found between different structures. Note also that the localized basis sets used are generally of modest quality. Regarding the anions, geometries are obtained at the semi-empirical AM1 level and energies are calculated in the HF approximation

[118] Poirier DM, Knupfer M, Weaver JH, Andreoni W, Laasonen K, Parrinello M, Bethune DS, Kikuchi K, Achiba Y. 1994. *Phys. Rev. B* 49:17403-11

[119] Kikuchi K, Nakahara N, Wakabayashi T, Suzuki S, Shiromaru H, Miyake Y, Saito K, Ikemoto I, Kainosho M, Achiba Y. 1992. *Nature* 357:142-44; Achiba Y, Kikuchi K, Aihara A, Wakabayashi T, Miyake Y, Kainosho M. 1995. *Mater. Res. Soc. Symp. Proc.* 359:3

[120] Rubin Y. 1997. *Chemistry – A European Journal* 3:1009-16, and references therein

[121] Prato M, Wudl F. 1995. *J. Am. Chem. Soc.* 117:7003-4

[122] An interesting proposal for the "opening" of C_{60} in the triplet state is given in Murry RL, Scuseria GE. 1994. *Science* 24:791-93. Calculated values, however, can only be considered rough estimates, as they are based on MNDO geometries, and the $T = 0$ calculations of the energy barrier in DFT-based calculations also use poor basis sets

[123] Blinc R, Pokhodina K, Cevc P, Arcon D, Omerzu A, Mihailovic D, Venturini P, Golic L, Trontelj Z, Luzuik I, Jeglicic Z, Pirnat J. 1996. *Phys. Rev. Lett.* 76:523-26; Bele P, Brunner H, Schilder A, Gmeiner J, Schwoerer M. 1997. *Adv. Mater.* 9:907-9

[124] Martin TP, Malinowski N, Zimmermann U, Näher U, Schaber H. 1993. *J. Chem. Phys.* 99:4210-12; Zimmermann U, Malinowski N, Näher U, Frank S, Martin TP. 1994. *Phys. Rev. Lett.* 72:3542-45; Tast F, Malinowski N, Frank S, Heinebrodt M, Billas IML, Martin TP. 1996. *Phys. Rev. Lett.* 77:3529-32

[125] Kohanoff J, Andreoni W, Parrinello M. 1992. *Chem. Phys. Lett.* 198:472-77

[126] Andreoni W, in Ref. [2c]

[127] Tast F, Malinowski N, Frank S, Heinebrodt M, Billas IML, Martin TP. 1997. *Z. Phys. D* 40:351-54

[128] Giannozzi P, Andreoni W. 1996. *Phys. Rev. Lett.* 76:4915-18

[129] Curioni A, Giannozzi P, Hutter J, Andreoni W. 1995. *J. Phys. Chem.* 99:4008-14

[130] Baumgarten M, Guegel A, Gherghel R. 1993. *Adv. Mater.* 5:458

[131] Andreoni W, Giannozzi P, Armbruster JF, Knupfer M, Fink J 1996. *Europhys. Lett.* 34:699-704

[132] Imahori H, Sakata Y. 1997. *Adv. Mater.* 9:537-46

[133] Gimzewski JK, in Ref. [2b], pp. 117-36

[134] see e.g. Cuberes CT, Schlittler RR, Gimzewski JK. 1996. *Appl. Phys. Lett.* 69:3016-18

[135] Rubin Y, in Ref. [2b], pp. 295-328

[136] Jensen AW, Wilson SR, Schuster DI. 1996. *Bioorg. Med. Chem.* 4:767-79

Table 1: C_{60}: Structural and electronic characteristics. 'v' and 'ad' denote vertical and adiabatic, respectively

	Bond lengths (Å)	IP (v) [IP (ad)] (eV)	EA (v) [EA (ad)] (eV)
LSD (P)[a]	1.387;1.438	7.59 [7.55]	2.90 [2.96]
LDA (AE)[b]	1.388;1.441	–	–
LDA (AE)[c]	1.39; 1.45	7.60	2.82
BLYP (P)[a]	1.401;1.459	7.08 [7.04]	2.47 [2.52]
BLYP (AE)[b]	1.403;1.461	–	–
exp[d]	1.401(10);1.458(6)[a]	7.6	2.65
HF[e]	1.370;1.448	8.0	0.65
HF[f]	1.372;1.448	–	–
MP2[g]	1.406;1.446		

[a]Ref. [6]
[b]Ref. [14] – TZP
[c]Ref. [15] – LCGTO (11s/7p/1d)
[d]Ref. [8]
[e]Ref. [7] – TZP
[f]J. Cioslowski, W. Thiel and S. Pachkovski, in [3], p. 51 – 6-311G*.
[g]Ref. [10] – TZP.

Table 2: C_{70}: Structural and electronic characteristics. d_1 to d_8: bond lengths in Å (Fig. 1(b)). Vertical and adiabatic values are reported for both IP and EA (in eV).

	LSD (P)[a]	BLYP (P)[a]	exp (GED)[b]	exp (SED)[c]	exp (ND)[d]	exp (XRD)[b]	exp	HF[h]	HF[i]
d_1	1.436	1.4565	1.461(8)	1.464(9)	1.460(4)	1.458(6)		1.451	1.452
d_2	1.389	1.403	1.388(17)	1.37(1)	1.382(6)	1.380(4)		1.375	1.370
d_3	1.433	1.453	1.453(11)	1.47(1)	1.449(5)	1.459(5)		1.446	1.447
d_4	1.383	1.397	1.386(25)	1.37(1)	1.396(6)	1.370(4)		1.361	1.356
d_5	1.431	1.451	1.468(11)	1.46(1)	1.464(7)	1.460(4)		1.457	1.458
d_6	1.425	1.444	1.425(14)	1.47(4)	1.420(4)	1.430(4)		1.415	1.414
d_7	1.409	1.426	1.405(13)	1.39(1)	1.415(5	1.407(7)		1.407	1.403
d_8	1.452	1.475	1.538(19)	1.41(4)	1.477(6)	1.476(5)		1.475	1.475
IP (v)	7.59	7.04					7.6 ± 0.1[f]	7.59	–
IP (ad)	7.54	7.00							
EA (v)	2.795	2.40					2.7 ± 0.1[g]	0.52	–
EA (ad)	2.86	2.46							

[a]Ref. [6]
[b]Ref. [24]
[c]Ref. [8]
[d]Ref. [25]
[e]Ref. [21]
[f]Ref. [27]
[g]Ref. [28]
[h][17] – STO-3G-DZP
[i][18] – 3-21G

Table 3: C_{60}: Calculated vibrational frequencies of the optically active modes in cm^{-1}

Mode	HF[a]	MP2[b]	LDA (P)[c]	BLYP (P)[c]	exp[d]
$T_{1u}(1)$			527	533	527 (527)
(2)			593	561	570 (576)
(3)			1231	1160	1170 (1183)
(4)			1511	1423	1407 (1429)
A_g	483	437	500	514	496(2)
	1614	1586	1546	1455	1470(2)
$H_g(1)$			251	243	271(2)
(2)			421	425	433(3)
(3)			712	702	710(2)
(4)			794	759	774(2)
(5)			1134	1084	1099(2)
(6)			1307	1224	1250(2)
(7)			1497	1411	1426(2)
(8)			1617	1544	1575(3)

[a]Ref. [7]

[b]Ref. [10]

[c]Ref. [6]

[d]Frequencies of Raman active modes are from Ref. [2a], p. 339, obtained from a fit to first-order and higher-order Raman spectra. Frequencies of IR active modes are from data on the gas phase [40]. The results of the same fitting procedure used for the Raman modes are given in parenthesis. For the specific publications, we refer the reader to Ref. [2a], Chapter 11.

Table 4: C_{70}: Calculated vibrational frequencies of IR active modes in cm^{-1}

Mode	LDA (P)[a]	BLYP (P)[a]	Mode	LDA (P)[a]	BLYP (P)[a]
$A_2''(1)$	322	323	$A_2''(6)$	1176	1121
(2)	464	463	(7)	1282	1189
(3)	584	563	(8)	1413	1306
(4)	721	720	(9)	1536	1439
(5)	944	901	(10)	1608	1532
$E_1'(1)$	326	329	$E_1'(12)$	1130	1067
(2)	366	359	(13)	1227	1165
(3)	420	416	(14)	1305	1227
(4)	516	508	(15)	1342	1266
(5)	552	530	(16)	1376	1300
(6)	588	580	(17)	1470	1385
(7)	650	647	(18)	1504	1405
(8)	687	678	(19)	1505	1407
(9)	824	800	(20)	1536	1453
(10)	842	833	(21)	1608	1530
(11)	933	897			

[a]Ref. [6]

Table 5: C_{60} dimers, neutral and charged: C–C bonds as in Fig. 3 and binding energy E_b with respect to the isolated monomers. Negative values mean that the dimer is not bound.

Method	d_1, d_2, d_3 (Å)	E_b (kcal/mol)
[2+2] isomer, doubly charged		
LDA (P)[a]	1.575, 1.573, 1.499	–21
LDA (AE)[b]	1.574, 1.584, 1.506	–3.5
BLYP (P)[a]	1.616, 1.613, 1.528	–52
B3LYP (AE)[b]	1.600, 1.608, 1.526	–34
HF (AE)[a]	1.580, 1.596, 1.521	–51
Singly bonded isomer, doubly charged		
LDA (P)[a]	1.611, 1.512, 1.493	–24
LDA (AE)[b]	1.582, 1.495, 1.524	–10
BLYP (P)[c]	1.677, 1.542, 1.521	–47.5
B3LYP (AE)[b]	1.606, 1.520, 1.540	-30
HF (AE)[b]	1.568, 1.524, 1.547	-17
[2+2] isomer, neutral		
LDA (P)[a]	1.578, 1.573, 1.498	11
LDA (AE)[b]	1.575, 1.585, 1.506	30
BLYP (P)[a]	1.620, 1.616, 1.530	–20
B3LYP (AE)[b]	1.594, 1.606, 1.525	–5 (+1)[d]
HF (AE)[a]	1.575, 1.594, 1.521	10

[a]Ref. [6]

[b]Ref. [67] – basis set is 3-21G

[c]First reported in [68]

[d]Ref. [67] – basis set is 6-31G* at the geometry obtained with the 3-21G basis.

Table 6: Calculated structural characteristics and binding energies for azafullerenes, in DFT–BLYP [6]. d_1 to d_4: bond lengths in Å. Notation according to Fig. 5 and comparable to that used for singly bonded $C_{120}^{(2-)}$ in Table 5. Note that for the latter, d_4 is 1.430 Å.

System	d_1	d_2	d_3	d_4	E_b (kcal/mol)	IP (ad) (eV)	EA (ad) (eV)
$C_{59}N$[a]	–	1.439	1.416	1.438		5.88	2.70
$(C_{59}N)_2$	1.609	1.550	1.520	1.425	15[b]	6.23	2.85
$C_{59}HN$	1.100	1.546	1.523	1.423	70[c]	6.59	2.48

[a]Changes with respect to Ref. [68] are due to a better convergence of the calculations reported here.

[b]Binding energy with respect to isolated $C_{59}N$

[c]Binding energy with respect to $C_{59}N$ and H

Table 7: Energy of different isomers of C_{82} and La@C_{82}. FM stands for the notation given in Ref. [116], p. 256. The chemisorption sites are defined according to the local configuration of the closest carbon neighborhood: "cora" stands for corannulene, whereas "green", "blue" and "red" indicate pyracylenes having two pentagons and six hexagonal rings around it (as in C_{60}), only one pentagon and seven hexagons, and only hexagons, respectively. All energies are in kcal/mol. B. E. is the binding energy of the complex. Reprinted from Ref. [115]. Copyright 1998 Springer-Verlag.

Cage (FM)	Energy	La@ site	Energy	B. E.
$C_2(3)$	0	green	22.5	78
		red	23	77
$C_2(5)$	5.5	blue	18.5	81
$C_2(1)$	8	green	26.5	87
$C_s(4)$	2	blue	28	74
$C_s(2)$	6.5	green	29	78
$C_s(6)$	8.5	blue	21	87
		cora	4.5	104
$C_{2V}(9)$	11	cora	0	111.5
		red	28.5	83
$C_{3V}(7)$	21.5	blue	27.5	94
$C_{3V}(8)$	22	blue	34	88

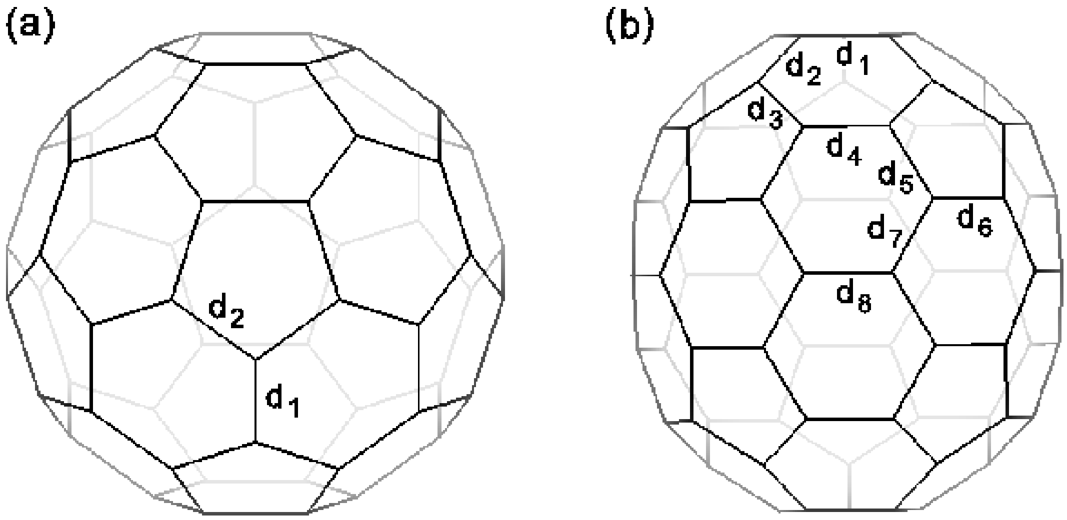

Figure 1: Structures of (a) C_{60} and (b) C_{70} with indication of the inequivalent bonds

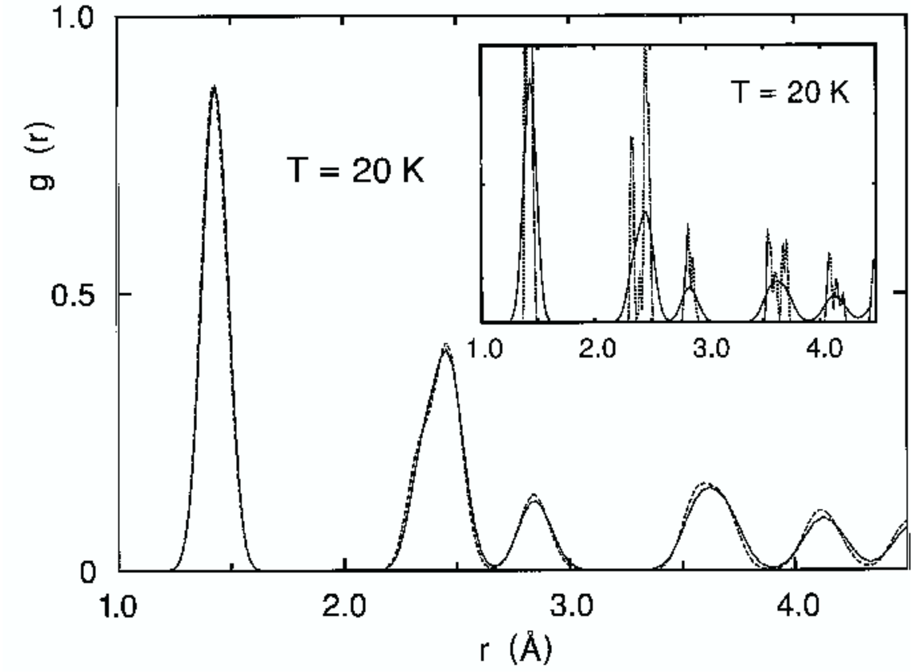

Figure 2: C_{70}: calculated quantum pair-correlation function (dashed curve) compared with experiment (solid line, from [25]). In the inset, the comparison is made with the classical pair-correlation function. Reprinted from [26], with kind permission from Elsevier Science – NL, Sara Burgerhartstraat 25, 1055 KV Amsterdam, The Netherlands

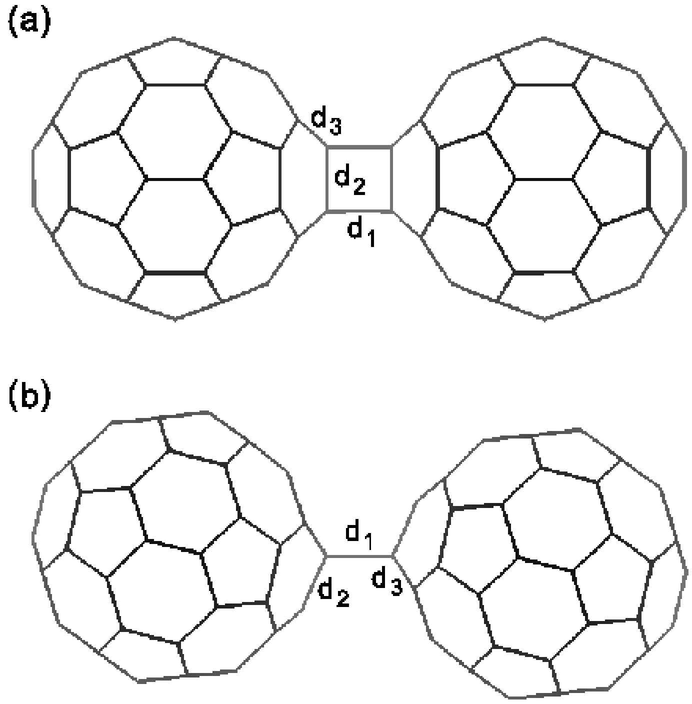

Figure 3: Two possible configurations of the C_{60} dimer: (a) [2+2] and (b) singly bonded anti-conformation

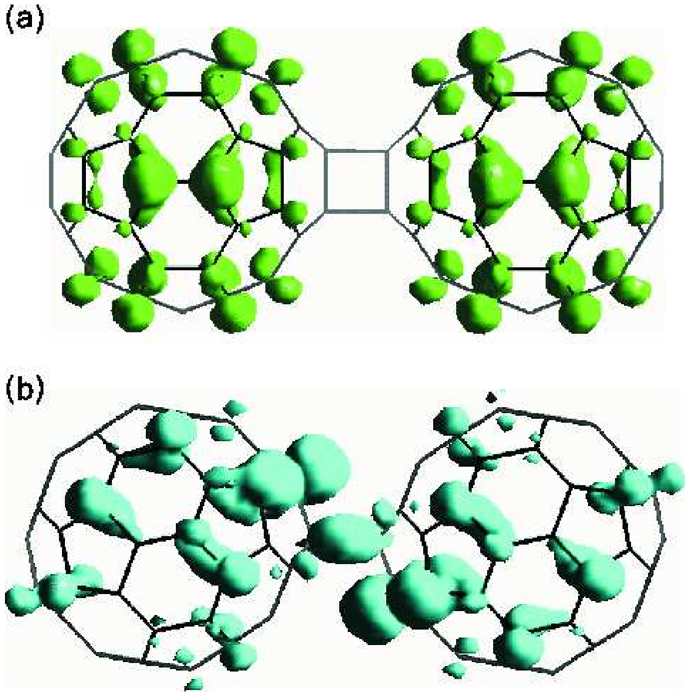

Figure 4: Electronic structure of the dimers: (a) and (b) HOMO of the doubly charged anions (isodensity surface = 0.0005 au)

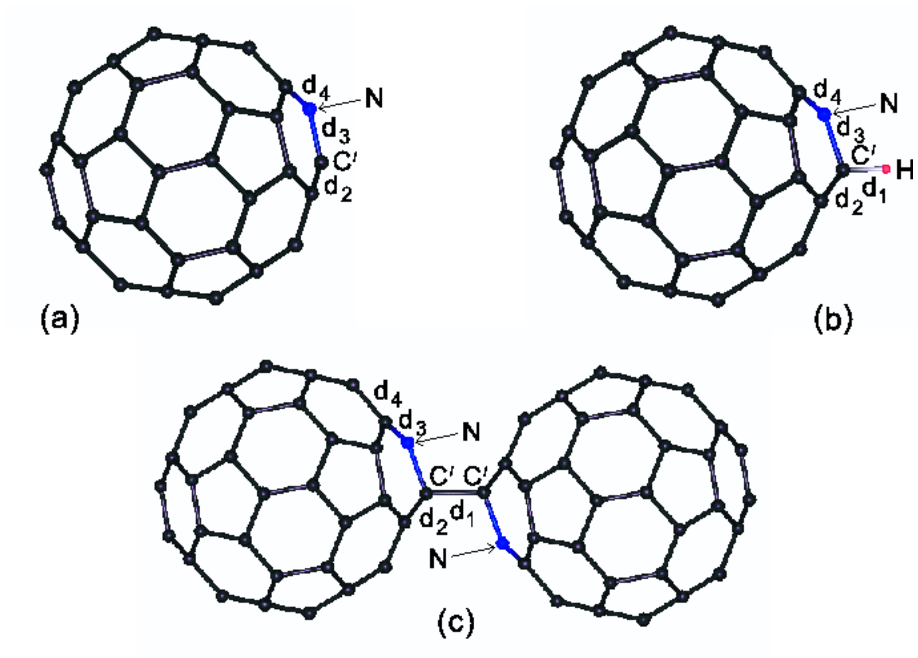

Figure 5: Azafullerenes: (a) $C_{59}N$, (b) $C_{59}HN$, and (c) $(C_{59}N)_2$

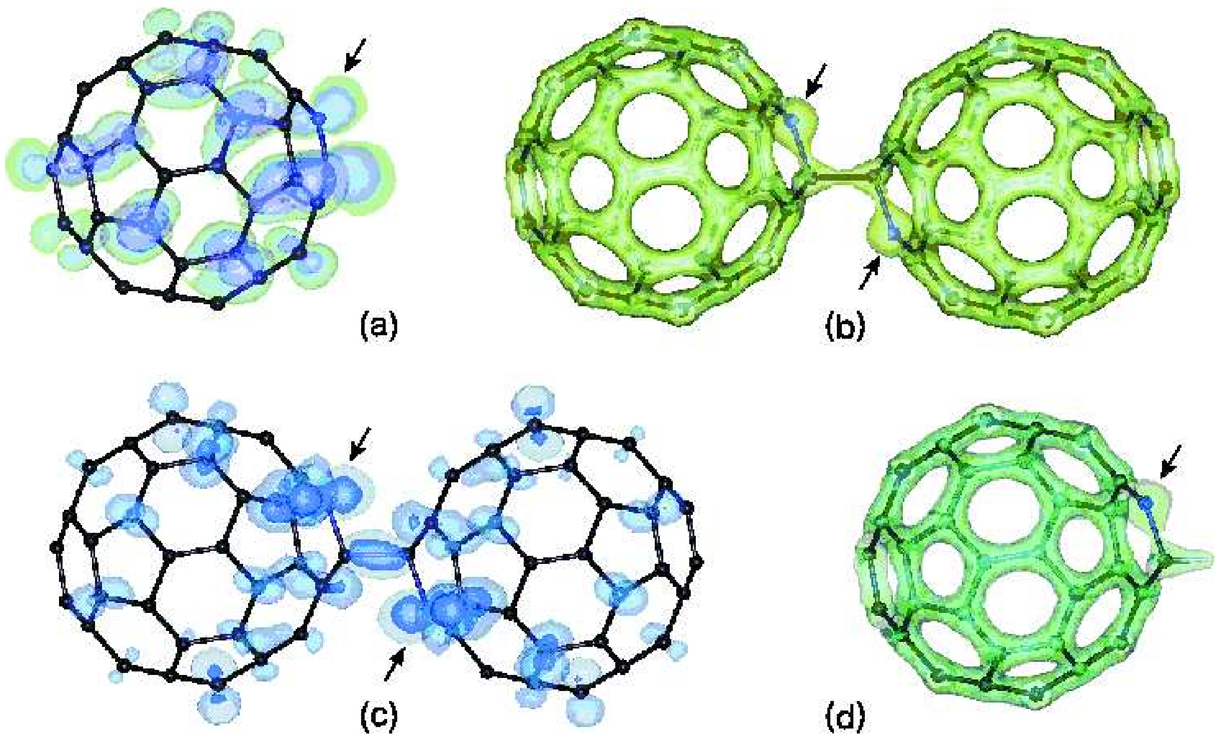

Figure 6: Electronic structure of the azafullerenes: isodensity hypersurfaces of (a) the electron spin density in $C_{59}N$ (0.001 and 0.0005 au); (b) and (d) the electron densities of $(C_{59}N)_2$ and $C_{59}HN$ (0.2 au); (c) the probability density of the HOMO in $(C_{59}N)_2$ (0.001 and 0.0005 au). Parts (b) and (c) are reprinted with permission from [68]. Copyright 1996 American Chemical Society

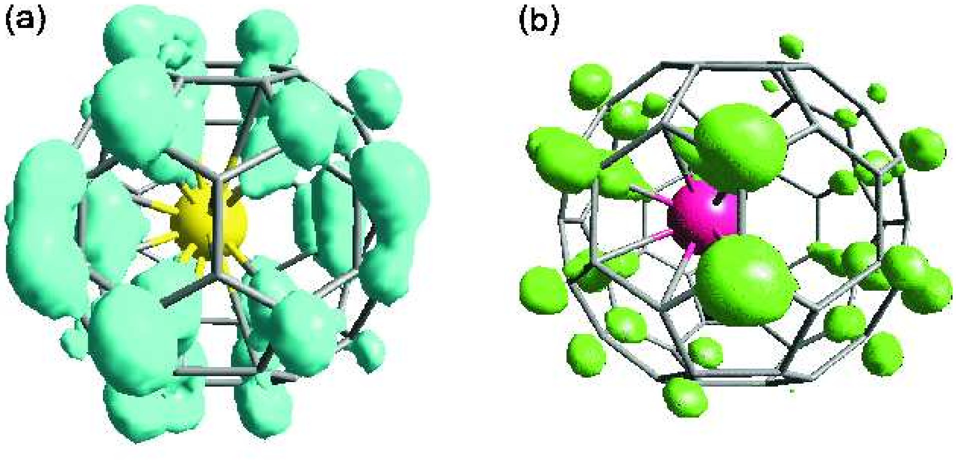

Figure 7: $La@C_{60}$ and $Li@C_{60}$: Electron spin densities (0.001 au). Reprinted from [115]. Copyright 1998 Springer-Verlag

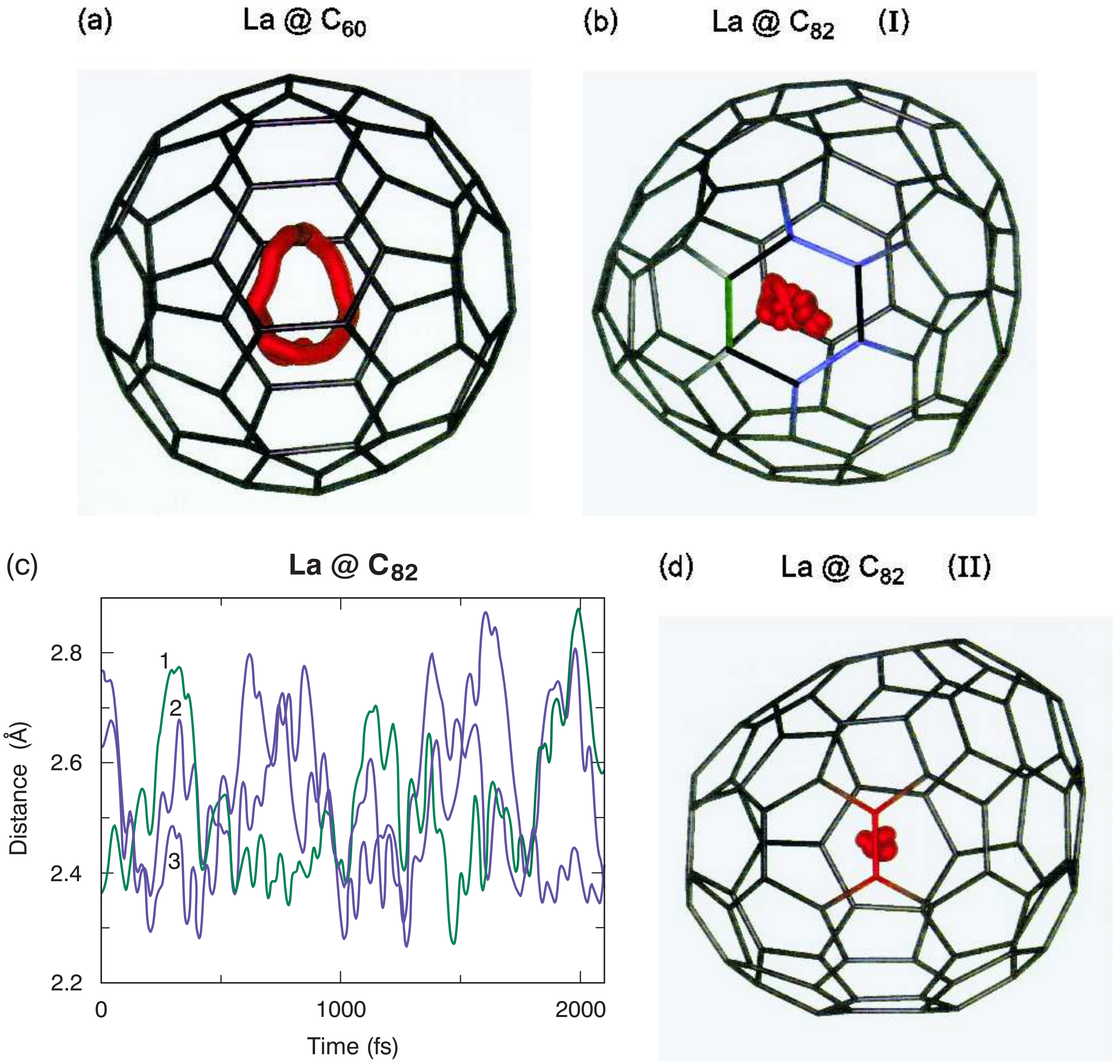

Figure 8: Dynamics of La@C_{60} and La@C_{82}. From [114]. Copyright 1996 The American Physical Society.

FROM: *Appl. Phys. A* (1998) in press

AB INITIO APPROACH TO THE STRUCTURE AND DYNAMICS OF METALLOFULLERENES

Wanda Andreoni and Alessandro Curioni

IBM Research Division, Zurich Research Laboratory, CH–8803 Rüschlikon, Switzerland

Abstract. We discuss the results of *ab initio* calculations of metallofullerenes carried out within density-functional-theory schemes. The systems considered in detail are both endohedral and exohedral complexes of lanthanum and lithium with C_{60} and La@C_{82}. Structural, electronic, and vibrational properties are determined and compared with experiment whenever possible. In the C_{60} case, clear characteristic and measurable features are found that distinguish between exo- and endo-complexes. Also in C_{82}, fingerprints for the presence of the guest atom, its position, and charge state are identified in measurable spectra, as well as of the structure of the cage.

1. Introduction

Compared to our knowledge of other fullerene derivatives, the understanding of the physics and chemistry of metallofullerenes has progressed slowly over the past ten years. This is the case even in spite of the recent proliferation of experiments and attempts to characterize them [1, 2]. In fact, there are still basic questions that are too difficult to answer from both experiment and theory or that have simply been ignored. For example, the endohedral nature of the metallofullerene under consideration has unambiguously been proved in only a few cases (see e.g. [3]). The (average) position of the metal atom(s) is (generally) unknown. Moreover, with the exception of C_{60} and C_{70}, there can be several options for the structure of the cage that experiments can rarely resolve. Also, the information one can obtain from experiment on the dynamical state of the metal atom(s) is limited to the time scale of conventional dynamical probes such as electron paramagnetic (EPR) or nuclear magnetic resonance (NMR).

It is clear that, in principle, calculations can be of great help in such a situation. One can unambiguously identify both similarities and discrepancies of exohedral and endohedral fullerene–metal complexes, and calculate structural and dynamical properties of any such system. However, the complexity of the problem should not be underestimated. For example, the structural problem itself requires both isocage and heterocage isomers to be considered. It is clear that an either inaccurate or incomplete search can be strongly misleading, and that reliable results require an *ab initio* and dynamical approach. This is especially true for a quantitative determination of relative stability and isomerization energies.

Here we report on investigations that we have carried out over the years, using density-functional-theory (DFT)-based molecular dynamics (MD) [4]. This approach has allowed us to explore the potential energy surface of metallofullerenes more thoroughly and also to go beyond a static modelization to study their dynamical and thermal behavior [5]. From our calculations, clear discrepancies emerge between the behavior of the endohedral and exohedral complexes that should be of help for their experimental characterization.

2. Density-functional-theory-based calculations

The calculations we describe here follow the DFT approach, within two different approximations for the exchange-correlation functionals with spin polarization: the local-spin-density one (LSD) [6] or that with gradient corrections of the Becke and Lee–Yang–Perdew type (B-LYP) [7]. Equations are solved explicitly only for the valence electrons, which interact with the core via angular-momentum-dependent pseudopotentials. In the case of La(Y), we consider eleven electrons in the valence shell, so as to allow the atomic 5s(4s) and 5p(4p) core states to relax as a consequence of the interaction with the carbon cage. These pseudopotentials are generated with the Martins–Troullier procedure [8], which can provide a good compromise between softness and transferability. The basis set for the electronic wave functions consists of plane waves [9], which allow a better and more controlled convergence than commonly used localized functions (see e.g. Refs. [10, 11]).

Optimization of the electronic wave functions is obtained with the DIIS algorithm [12, 13]. This is also used for local optimizations of the atomic coordinates, combined with a quasi-Newtonian optimization method [13]. It is worth emphasizing that our procedure is much more flexible than the ones commonly used in this field [10] because no symmetry constraint must be imposed. The harmonic vibrational frequencies corresponding to the motion at the local minima are calculated from finite differences.

Both the dynamical search for low-energy structures and the determination of the dynamical behavior is performed using DFT-based Car–Parrinello MD [4]. In particular, from the velocity–velocity autocorrelation function we determine the vibrational spectrum that now also contains anharmonic effects. Isomerization processes, which cannot be observed to occur spontaneously within the time of a free dynamics simulation, are studied with Car–Parrinello MD combined with the method of constraints [14]. This method [15] allows one to determine possible reaction paths *ab initio* and calculate free energy activation barriers by constraining suitable (one or more) geometrical variables of the system (reaction coordinates). We have applied it to La@C_{82} to investigate the dynamics of isomerization with La inside one specific cage.

3. Metallofullerenes based on C_{60}

3.1. Endohedral complexes

The first C_{60}-based metallofullerenes were discovered in molecular beams almost simultaneously with C_{60} itself [16]. However, none of the conventional ways of producing metallofullerenes has so far succeeded in separating one with C_{60} as cage in macroscopic quantities. Owing to the large availability of the bare fullerene compared with any of the others, such an achievement would ensure the realistic possibility of creating new solid phases with a variety of electronic and magnetic properties at least as rich as that obtained with intercalation. By bombarding C_{60} with alkali-metal ions, Campbell *et al.* have succeeded only very recently [17] in creating endohedrals.

Calculations of C_{60} with metal atoms incorporated are also relatively "old" by now and have gone through a number of steps [18]. *Ab initio* MD showed for the first time [19, 20] that the energetically favorable positions for the metal atom were off-center. Qualitatively, this can be understood at various levels. Acting as an electron donor to the threefold degenerate t_{1u} states of C_{60}, the metal atom induces a Jahn–Teller splitting that drives it away from the center. If we model the cage as a spherical electronic shell, its polarization will be the off-center driving mechanism, and the distance from the carbon shell will depend on the size and charge of the metal ion [21]. If we now allow for the dishomogeneity of the charge distribution and consider the specific bond pattern of the fullerene, we understand that the electron-rich regions, namely the "double bonds", will act as the attraction centers for the metal ion [22]. Depending on its charge, its size and its propensity to form a directional bond with the carbons, the guest atom will position itself more or less away from the center of the pyracylene unit surrounding the double bonds. Owing to the delocalized character of the t_{1u} states, additional effects resulting from the distribution of the excess charge density are minor.

With this scheme in mind, we can now consider our results on two specific and distinct cases: La@C_{60} and Li@C_{60}. The electronic configuration of the lanthanum atom is [Xe]$5d^1 6s^2$, whereas that of Li is $1s^2 2s$. Clearly their binding with carbon is generally very different. In the endohedral complexes with C_{60}, both essentially act as electron donors. Their $T = 0$ position inside the cage is shown in Fig. 1, together with the distribution of the spin density. The chemisorption site for La closely corresponds to the center of the pyracylene unit, with a first coordination of six and distances in the range of 2.55–2.64 Å [23]. Lanthanum is strongly ionized and to a first good approximation can be considered in the 3+ charge state. This bonding deforms the cage locally in a sizable manner, with an elongation of the "double-bond" lengths up to 0.07 Å. Owing to the difference in size and valency, lithium comes closer to the center of the hexagon, and deforms the cage to a lesser extent. The closest shell is composed by six atoms at distances in the range 2.16–2.22 Å and the elongation of the pyracylene double bonds is of 0.03 Å. The calculated binding energy is about $\sim$61 kcal/mol for La and $\sim$44 kcal/mol for Li [23].

Figure 1 shows the spin density, namely the probability distribution of the unpaired electron that EPR experiments can detect. In both cases, it is delocalized on a large portion of the cage but with largest amplitude in the close environment of the metal atom. However, care must be taken in drawing conclusions about the chemical bonding from the knowledge of the spin density, which does not necessarily reflect it. For instance, inspection of the electron density as well as the projected density of states (PDOS) (Fig. 2) reveals that the metal atom is not a "simple" electron donor. Only the 5s core states are quite insensitive to the interaction with the cage (a sharp peak in Fig. 2), whereas the 5p core polarizes strongly, and a weak contribution from the 5d orbitals is present below the highest occupied molecular orbital. In the case of Li@C_{60}, the projection of the DOS on lithium is negligible, consistent with full electron transfer to the cage.

Car–Parrinello LSD–MD simulations of La@C_{60} [22] show that at least at room temperature the static picture is not appropriate. Figure 3 shows the picture resulting from the La trajectories. It takes it only 1.1 psec to go "full circle" inside the cage. The metal atom diffuses rapidly from one minimum to the next, passing through the connecting pentagonal rings. During this motion, it keeps its distance from the carbon shell constant within 0.2 Å and the coordination close to six [24]. The vibrational spectrum we obtain from the velocity–velocity autocorrelation function bears fingerprints of the presence of lanthanum and also of its "spatially limited diffusion". In fact, all modes involving lanthanum are much lower in energy than those of C_{60}, and vibrational density is appreciable down to about 30 cm^{-1}.

In the case of lithium, analogous simulations at room temperature show that the residence times on the minima are one order of magnitude longer. The positions of two consecutive minima are farther apart than in the case of lanthanum.

3.2. Exohedral complexes and comparison with endohedrals

Figure 4 illustrates the exohedral complexes for lanthanum and lithium, and the distribution of the unpaired electron.

In the case of La, both the spin density [Fig. 4(a) and Fig. 1(a)] and the (P)DOS (Fig. 2) show a strong discrepancy between LaC_{60} and $La@C_{60}$. The reason lies in the different valency of lanthanum. In fact, when it is outside the cage, the 5d electron is not ionized but hybridizes strongly with the C_{60} orbitals. To a good approximation, it can be considered in the 2+ charge state. This result agrees with indications from experiments on epitaxially grown multilayers with a 1:1 composition of lanthanum and C_{60} [25]. In the exohedral configuration, lanthanum is slightly displaced from the center of the hexagon. Thus its first coordination shell still contains six atoms, with distances in the range of 2.64–2.73 Å [23]. The binding energy [23] is lower by 10 kcal/mol than in the endohedral configuration.

A sizeable difference in the bonding seems to exist also for the case of lithium, which is closer to the carbon shell. Also the spin density shows this quite clearly: On the atoms around lithium, it is strongly polarized towards it. Contrary to the case of lanthanum, the binding energy is by 7 kcal/mol higher than in the endohedral configuration [23]. The six Li–C close neighbors are at distances of 2.23–2.32 Å [23].

For the case of lithium fullerenes, we have also calculated the IR spectrum, as shown in Fig. 5. This corresponds to the LSD optimization and to harmonic frequencies. Above 500 cm^{-1} one can still well recognize the C_{60} modes in both cases as well as the activation of essentially the same new modes. In contrast, the difference in the low-frequency side of the spectrum is striking. In fact, below 500 cm^{-1}, new modes of the cage become dipole allowed in both cases, but much more strongly so in the exohedral complex. This feature could be used to detect the presence of one relative to the other complex from experiment.

4. $La@C_{82}$: iso- and hetero-cage isomers

Following Fowler and Manolopoulos [26], there are nine isolated-pentagon isomers of C_{82}, of which three have C_2 symmetry (82:1; 82:3; 82:5), three C_s (82:2; 82:4; 82:6), two C_{3V} (82:7 and 82:8) and one C_{2V} (82:9). NMR experiments identify C_2 as the symmetry of the most commonly observed structure of C_{82} [27]. Calculations performed at different levels of sophistication are consistent with this finding, and agree in defining the 82:3 structure as the ground state and the C_{3V} isomers as the top of the energy scale. The ordering of the others is a more delicate question, and requires accurate calculations to be established. In Table 1, we report the relative energies of these isomers calculated in DFT–BLYP.

In ignorance of the cage structure in the complexes, the 82:3 is the one commonly considered also in the theoretical studies of lanthanum and yttrium endohedrals [10, 22, 28] and for the interpretation of experiments (see e.g. [3, 28]). In earlier calculations [10, 28] the metal atom was positioned on the symmetry axis. Progress was made only a few years later, using DFT–LSD-based MD for the search of the preferred endohedral configurations [22]. This yielded unforeseen structures and showed that all previous predictions for the energetically favored chemisorption sites were too high to be probable geometries at room temperature. In particular, the lanthanum position on the C_2 axis turned out to be ~13 kcal/mol higher than the ground state. The energetically favored chemisorption sites obtained in this way have helped us understand the general criteria leading to the most probable configurations of encapsulated electron donors. As discussed in the previous section, double bonds are the center of attraction for the metal ions. On passing from C_{60} to higher fullerenes, one realizes that this type of double bonds can still be identified, namely the centers of the pyracylene units, which however are generally inequivalent. In fact, if one considers just the first neighboring rings, see Fig. 6, they can be classified into three types, which we call "green" (close environment as in C_{60}), "blue" (only one pentagon and seven hexagons) and "red" (only hexagons) [29]. In the

82:3 cage, only the positions corresponding to the "green" [Fig. 7(a)] and "red" pyracylenes are minima of the potential energy surface and very close in energy (see Table 1).

We have recently extended our investigation to the other cages. The results obtained so far are reported in Table 1. Note that these are still *partial* because only local minimization was performed starting from different configurations of the metal atom, and not a full dynamical search. There is no doubt, however, that La@C_{82} complexes have a different energetics than bare C_{82} does, as anticipated in Ref. [28]. Also, the C_{2V} and one of the C_s(82:6) cages are by far preferred by La over the 82:3 one (by about 20 kcal/mol). This unambiguously shows that determining *a priori* which is the energetically most stable La–fullerene complex is not trivial, because several factors must be included: the propensity of the cage to "receive three electrons", the relative stability of the bare molecular isomer, the type of binding allowed by a specific geometry, and the distribution of the molecular orbitals that act as acceptors. Through specific calculations also of molecular anions, we have verified that none of these criteria is sufficient by itself. We emphasize that the energy differences of the different isomers cannot be determined meaningfully if the relaxation of the carbon shell associated with the formation of the metal bonding is ignored. These results will be explained in detail elsewhere.

Let us consider here the C_{2V} case. Its triply charged anion is the lowest in energy. Concerning pyracylene units, there are only two inequivalent ones, both of the red type. When La is positioned there, the energy of the complex belongs to the same range as that of the other cages with lanthanum in one of the blue, green or red positions. However, the C_{2V} structure allows an unsuspected chemisorption site [see Fig. 7(b)] that is near the symmetry axis, with a corannulene-like environment ("cora"), where the binding is much stronger than in all other configurations. This is related to the fact that the lowest unoccupied orbitals of the bare fullerene (the acceptor states) are confined to this region, and allow a stronger metal–cage coupling.

A clear message of these calculations is that the structure of the cage in the various experiments conducted so far may well be different. Having one or the other type of cage, or a mixture of them, will depend on the production mechanism, namely on kinetic as well as energy factors.

It is interesting to see how quantities that are experimentally accessible, such as the spin density distribution [30] and the photoemission response, depend on the specific isomer. Figure 8 shows the DOS (above) and its projection on the lanthanum states (below) for the 82:3 and 82:9 cases. Discrepancies between the carbon-related features of the two structures are evident. Regarding the projection on lanthanum, similar comments can be made as for La@C_{60} (Sect. 3.1). Moreover, a significant dependence on the specific geometry appears, especially concerning the 5d contribution. This is particularly interesting in view of recent resonant photoelectron spectroscopy measurements that have been interpreted as sign of incomplete charge transfer from lanthanum [31].

Within a given cage, distinct chemisorption sites are possible, which are separated by energy differences of the order of the kcal/mol (Table 1). It is interesting to see to what extent and how the metal atom moves inside the molecule. In Ref. [22], we have studied this question with *ab initio* MD simulations for the C_{82} (82:3) cage. Contrary to the case of C_{60}, the motion is not diffusive but remains confined around the minima. This is shown in Fig. 9. In (a) the carbon structure around La is of the "green" type and consists of five fused pyracylene units. This permits greater freedom for the moving lanthanum than in the "red" one (b), so that the motion in this valley is complex and residence times are at most of the order of 0.1 psec. Using LSD-based MD with constraints, also at room temperature, we have determined a possible dynamical path for the isomerization and calculated the relative free energy barrier. The lanthanum atom moves from the higher minimum (red) to the ground state (green) in a way similar to that of the diffusion inside C_{60}, namely, it has to go through configurations in which it is more closely coordinated to the pentagonal rings. Broadly speaking, these determine the barriers for its motion. Our calculated value of the free energy barrier at room temperature is about 10 kcal/mol. This is consistent with the elusive isomerization in free MD at room temperature. Such a value is at least a factor of two higher than the relative energy of different iso- and hetero-cage isomers. Note that the simulation refers to the isolated molecule and that such a quantity will be sensitive to the environment.

In spite of the presence of anharmonic effects characterizing the lanthanum motion, it is interesting to determine the harmonic vibrational spectrum of the metallofullerene and compare it to that of the empty fullerene. In fact, in this way, the salient characteristics of the vibrations can be obtained and the special effects of the endohedral doping identified. We have calculated the infrared spectrum (Fig. 10) for the 82:3 case. The main features are the following: an overall intensity increase of the cage spectrum due to electron transfer from the metal atom, the presence of new modes in the far infrared that are associated with the metal atom (already identified in our analysis of the dynamical trajectories [22]), and the relatively strong enhancement and red shift of specific tangential modes of the cage. We have verified that the C_{82} tangential vibrations can be classified in terms of the three types of pyracylene units. In particular, the most strongly affected and enhanced amongst the infrared active modes are those involving the pyracylenes around the metal atom. These strongly relax as a consequence of the interaction with it, and there the excess electron density is more confined. Therefore, the extension of such calculations to other cages should help to interpret the experimental spectra, if measured at low temperature. For the moment, the published experimental spectra [32, 33] are not easily comparable amongst themselves, and probably suffer from the coexistence of the different isomers.

5. Conclusions

In this paper, we have summarized the results of DFT-based calculations of metallofullerenes having C_{60} as cage, and of the most experimentally studied endohedral complex of higher fullerenes: La@C_{82}. First, we emphasize that accurate *ab initio* calculations are crucial for a sensible assessment of their energetics. In particular, this requires a correct account of the changes the guest–host interaction induces in the geometrical and electronic structure of the cage.

In the case of C_{60}, contrasting endohedral and exohedral complexes has revealed important discrepancies in their electronic and vibrational properties. These could be used to experimentally distinguish whether one or the other is present using either photoemission or infrared spectroscopies, and thus be of help in the search for an unambiguous characterization of the nature of the available C_{60} complexes.

The case of La@C_{82} exemplifies all the problems a theoretical *a priori* study must solve for the case of higher fullerenes, where both isocage and heterocage isomers may be energetically competitive. Both electronic and vibrational spectra are sufficiently sensitive to distinguish the difference isomers. However, currently comparison with experiment cannot be carried out to complete satisfaction. In fact, in the real samples the presence of different and/or several isomers is possible. A higher population of one or the other depends on the preparation conditions. The importance of molecular dynamics simulations is amply shown, both as an optimization procedure and for the correct determination of the behavior of the guest atom at room temperature. We have presented here our results for the isomerization reaction in one cage. Extension of these calculations to other cages and further to other systems as well as a careful reconsideration of recent experiments are desirable.

References

[1] *Proc. Euroconf. on Electrical Properties of Novel Materials: Fullerenes and Fullerene Nanostructures*, Kirchberg, Austria, March 2-9, 1996, ed. by H. Kuzmany, J. Fink, M. Mehring, S. Roth (World Scientific, Singapore, 1996)

[2] *Recent Advances in the Chemistry and Physics of Fullerenes and Related Materials*, Vol. **4**, ed. by K.M. Kadish, S.R. Ruoff, (Electrochemical Society, Inc., Pennington, NJ, 1997)

[3] M. Takata, B. Umeda, E. Nishibori, M. Sakata, Y. Saito, M. Ohno, H. Shinohara: Nature **377**, 46 (1995)

[4] R. Car, M. Parrinello: Phys. Rev. Lett. **55**, 2471 (1985)

[5] The MD runs at constant temperature are carried out using the Nosé–Hoover method, see S. Nosé: J. Chem. Phys. **81**, 541 (1984) and W.G. Hoover: Phys. Rev. A **31**, 1695 (1985)

[6] We use the parametrization given in J.P. Perdew, A. Zunger: Phys. Rev. B **23**, 5048 (1981)

[7] A. Becke: Phys. Rev. A **38** 3098 (1988); C. Lee, W. Yang, R.G. Parr: Phys. Rev. B **36**, 785 (1988)

[8] N. Troullier, J.L. Martins: Phys. Rev. B **46**, 1754 (1992)

[9] For the isolated clusters, we used the method introduced in R.N. Barnett, U. Landman: Phys. Rev. B **48**, 2081 (1993)

[10] S. Nagase, K. Kobayashi, T. Kato, Y. Achiba: Chem. Phys. Lett. **201**, 475 (1993); *ibid.* **214**, 57 (1993)

[11] L.S. Wand, J.M. Alford, Y. Chai, M. Diener, J. Zhang, S.M. McClure, T. Guo, R.E. Smalley: Chem. Phys. Lett. **207**, 354 (1993)

[12] P. Pulay: Chem. Phys. Lett. **73**, 393 (1980)

[13] J. Hutter, H.P. Lüthi, M. Parrinello: Comput. Mat. Sci. **2**, 224 (1994)

[14] E.A. Carter, G. Ciccotti, J.T. Hynes, R. Kapral: Chem. Phys. Lett. **156**, 472 (1989)

[15] A. Curioni, M. Sprik, W. Andreoni, H. Schiffer, H. Hutter, M. Parrinello: J. Am. Chem. Soc. **119**, 7218 (1997)

[16] J.R. Heath, S.C. O'Brien, Q. Zhang, Y. Liu, R.F. Curl, H.W. Kroto, F.K. Tittl, R.E. Smalley: J. Am. Chem. Soc. **107**, 779 (1985)

[17] R. Tellgmann, N. Krawez, S.-H. Lin, I.V. Hertel, E.E.B. Campbell: Nature **382**, 407 (1996)

[18] J. Ciosloxwski: *Electronic Structure Calculations on Fullerenes and Their Derivatives*, Chap. 8 (Oxford University Press, New York, 1995)

[19] K.E. Laasonen, W. Andreoni, M. Parrinello: Science **258**, 1916 (1992)

[20] W. Andreoni, A. Curioni: In *Progress in Fullerene Research*, ed. H. Kuzmany, J. Fink, M. Mehring, S. Roth (World Scientific Publishers, Singapore, 1994), p. 93. In particular, LDA results are reported here for Me@C_{60}, with Me = Na, K, Al, La, and Y.

[21] S.C. Erwin: In *Buckminsterfullerenes*, ed. by W.E. Billups, M.A. Ciufolini (VCH Publishers, New York, 1993), p. 217

[22] W. Andreoni, A. Curioni: Phys. Rev. Lett. **77**, 834 (1996)

[23] Structures and energies refer to very recent calculations carried out in the spin-polarized BLYP approximation that are more accurate than the LSD, especially for the binding energies. The reported IR spectra refer to LSD calculations.

[24] W. Andreoni, A. Curioni: In *The Chemical Physics of Fullerenes 10 (and 5) Years Later*, ed. by W. Andreoni, NATO ASI Series E: Applied Sciences, Vol. **316**, (Kluwer, Dordrecht, 1996), p. 183

[25] C. Cepek, M.R. Hunt, A. Goldoni, S. Prato, S. Modesti: in Ref. [1], p. 284

[26] P.W. Fowler, D.E. Manolopoulos: *An Atlas of Fullerenes* (Clarendon Press, Oxford, 1995), p. 256

[27] K. Kikuchi, N. Nakahara, T. Wakabayashi, S. Suzuki, H. Shiromaru, Y. Miyake, K. Saito, I. Ikemoto, M. Kainosho, Y. Achiba: Nature **357**, 142 (1992); Y. Achiba, K. Kikuchi, A. Aihara, T. Wakabayashi, Y. Miyake, M. Kainosho: Mater. Res. Soc. Symp. Proc. **359**, 3 (1995)

[28] D.M. Poirier, M. Knupfer, J.H. Weaver, W. Andreoni, K. Laasonen, M. Parrinello, D.S. Bethune, K. Kikuchi, Y. Achiba: Phys. Rev. B **49**, 17403 (1994)

[29] In the 82:3 structure, the number of double bonds of the green, blue, and red type is two, eight, and four, respectively.

[30] D.S. Bethune, R.D. Johnson, J.R. Salem, M.S. deVries, C.S. Yannoni: Nature **366**, 123 (1993)

[31] B. Kessler, A. Bringer, S. Cramm, C. Schlebusch, W. Eberhardt, S. Suzuki, Y. Achiba, F. Esch, M. Barnaba, D. Cocco: Phys. Rev. Lett. **79**, 2289 (1997)

[32] R.H. Michel, R.D. Beck, A. Fischer, F. Hennrich, P. Weis, D. Fuchs, G. Bräuchle, S. Richard-Schneider, M.M. Kappes: In: *The Chemical Physics of Fullerenes 10 (and 5) Years Later*, ed. by W. Andreoni, NATO ASI Series E: Applied Sciences, Vol. **316**, (Kluwer, Dordrecht, 1996), p. 149

[33] K. Kikuchi, S. Suzuki, Y. Nakao, N. Nakahara, T. Wakabayashi, H. Shiromaru, K. Saito, I. Ikemoto, Y. Achiba: Chem. Phys. Lett., **216**, 67 (1993)

[34] W. Andreoni, A. Curioni: in Ref. [2], p. 516

Table 1. Energy of different isomers of C_{82} and La@C_{82} (see text). FM stands for the notation from Ref. [26]. All energies are in kcal/mol. B. E. is the binding energy of the complex.

Cage (FM)	Energy	La@-site	Energy	B. E.
$C_2(3)$	0	green	22.5	78
		red	23	77
$C_2(5)$	5.5	blue	18.5	81
$C_2(1)$	8	green	26.5	87
$C_s(4)$	2	blue	28	74
$C_s(2)$	6.5	green	29	78
$C_s(6)$	8.5	blue	21	87
		cora	4.5	104
$C_{2V}(9)$	11.	cora	0	111.5
		red	28.5	83
$C_{3V}(7)$	21.5	blue	27.5	94
$C_{3V}(8)$	22	blue	34	88

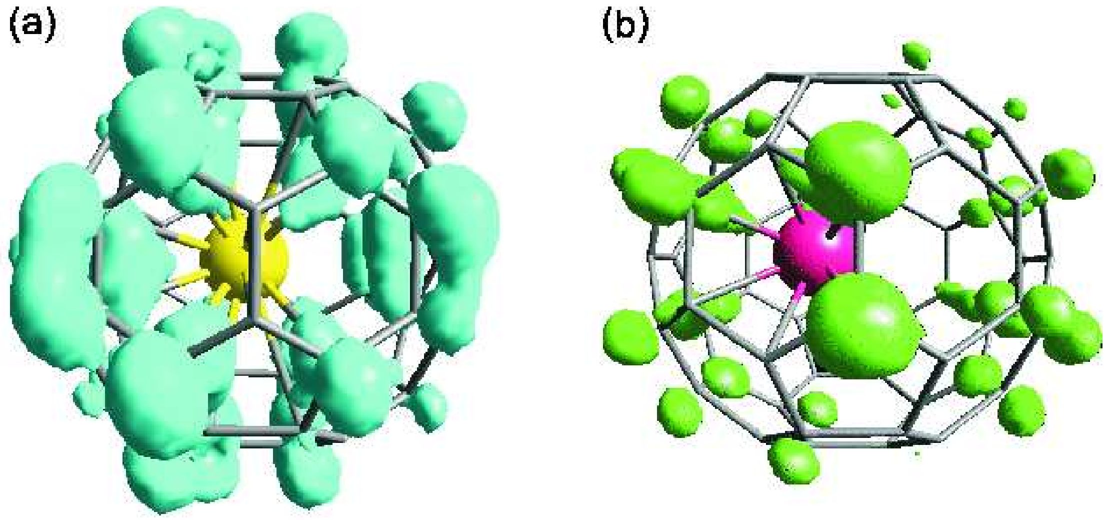

FIG. 1. (a) La@C_{60} and (b) Li@C_{60}: electron spin density (from [34]). The illustrated hypersurface corresponds to the value 0.001 e/(au)^3.

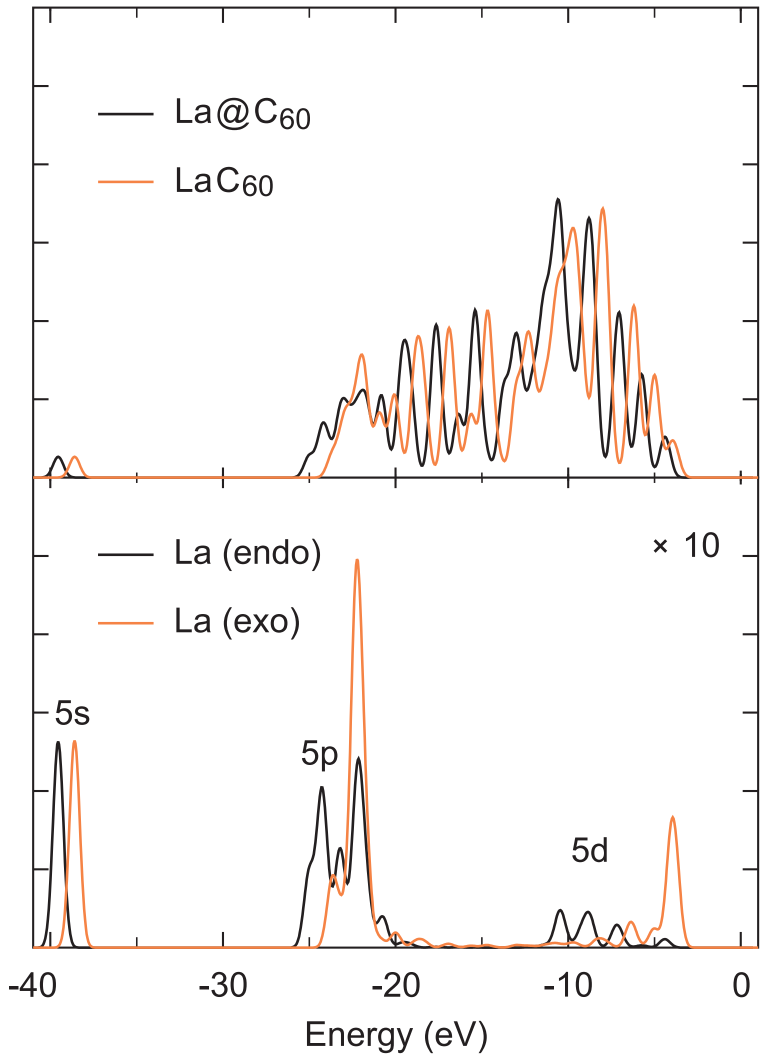

FIG. 2. La@C_{60} and LaC_{60}: density of the occupied electron states (above) and its projection on lanthanum (below).

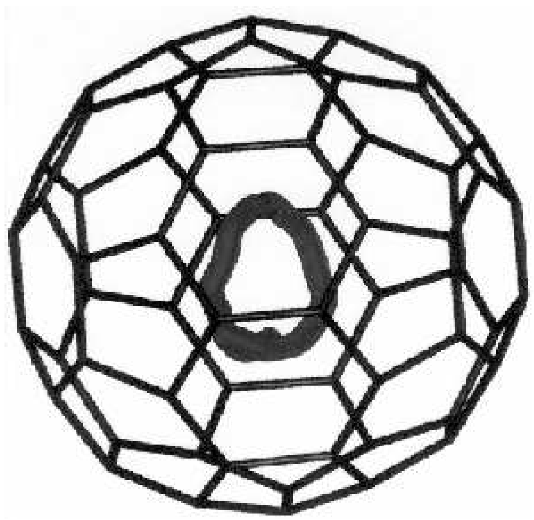

FIG. 3. La@C_{60}: room-temperature trajectory of La, taken over 1.1 psec. From [22].

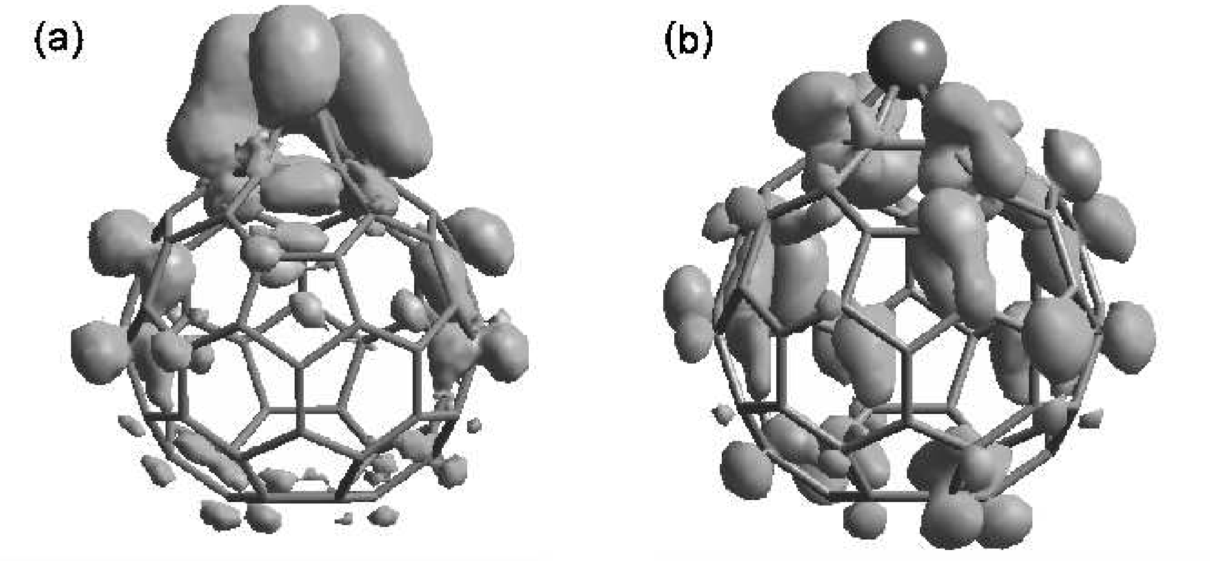

FIG. 4. (a) LaC_{60} and (b) LiC_{60}: electron spin density. The illustrated hypersurface corresponds to the value 0.001 e/(au)^3.

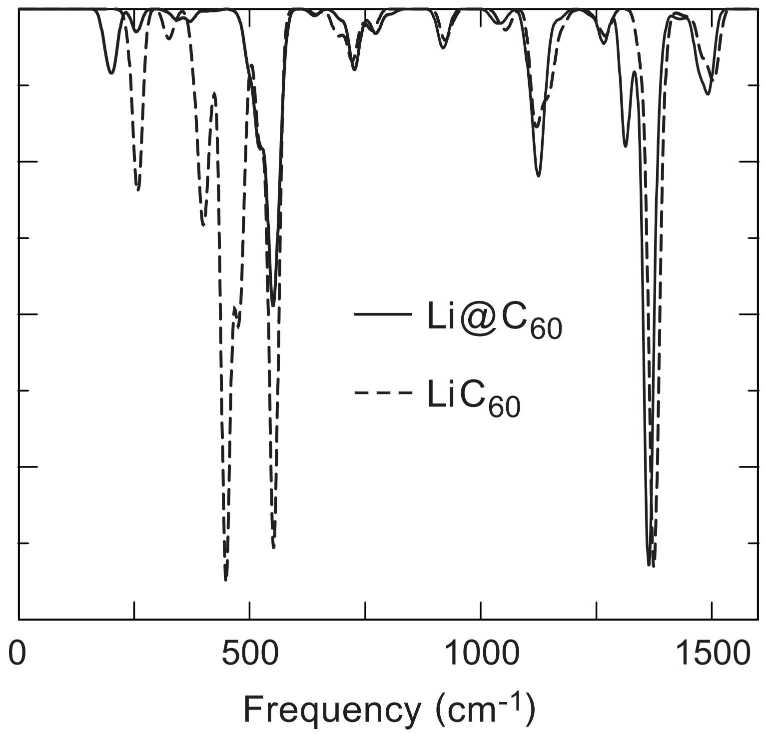

FIG. 5. Li@C_{60} and LiC_{60}: calculated infrared spectra.

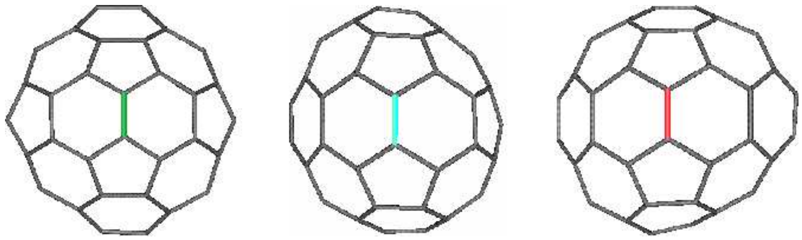

FIG. 6. Classification of pyracylene units in fullerenes other than C_{60}. From left to right: green, blue, and red. From [22].

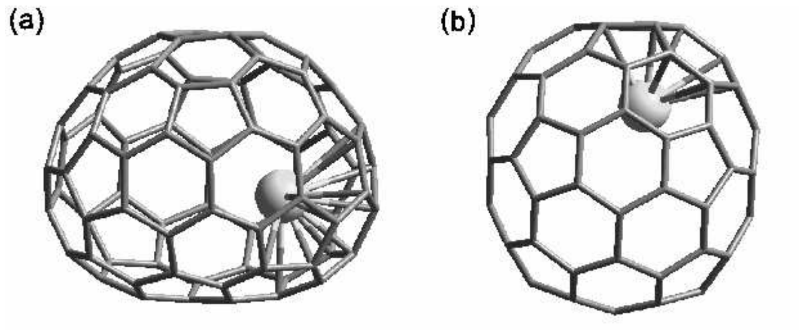

FIG. 7. La@C_{82} in (a) the 82:3 and (b) the 82:9 cage (see text).

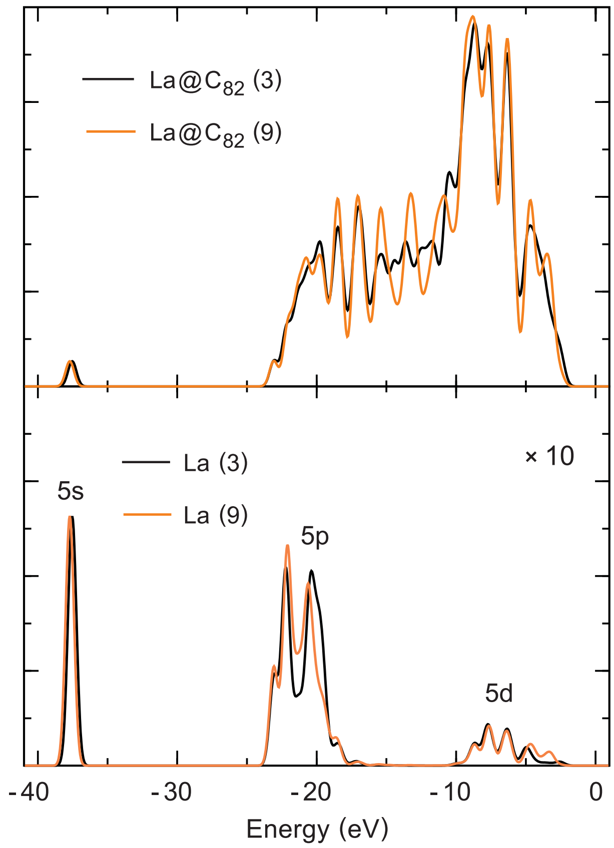

FIG. 8. La@C_{82}: density of the occupied electron states (above) and its projection on lanthanum (below) for the 82:3 and the 82:9 cage (see text).

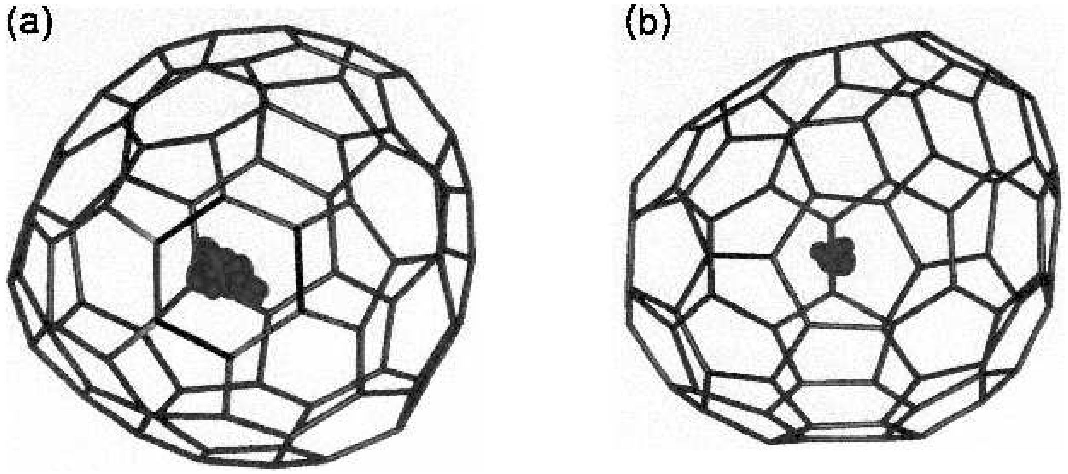

FIG. 9. La@C_{82} in the 82:3 cage: room-temperature trajectory of La around (a) the green and (b) the red chemisorption sites, taken over 2 psec. From [22].

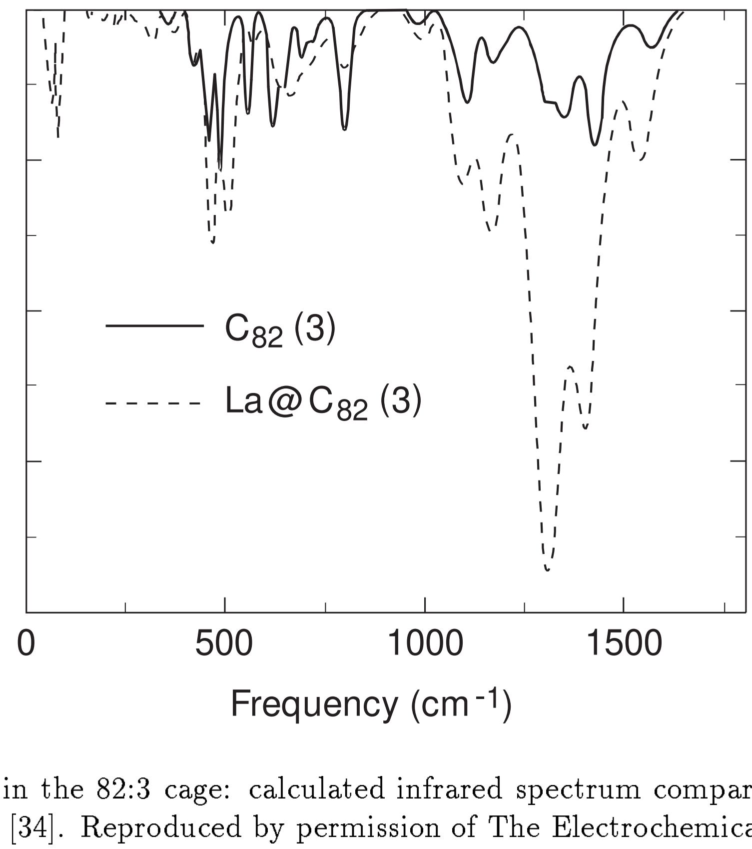

FIG. 10. La@C_{82} in the 82:3 cage: calculated infrared spectrum compared with that of the empty cage. From [34]. Reproduced by permission of The Electrochemical Society, Inc.